This is to certify that the

thesis entitled

Three-Dimensional Dynamic Motion of
the Shoulder Complex
presented by

Tamara Ann Reid

has been accepted towards fulfillment
of the requirements for

M.S. degree in Mechanics

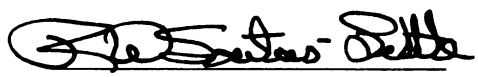

Major professor

Date Mar 28, 1994

THREE - DIMENSIONAL DYNAMIC MOTION OF THE SHOULDER COMPLEX

By

Tamara Ann Reid

A THESIS

Submitted to
Michigan State University
in partial fulfillment of the requirements
for the degree of

MASTER OF SCIENCE

Department of Material Science and Mechanics

1994

ABSTRACT

THREE-DIMENSIONAL DYNAMIC MOTION OF THE SHOULDER COMPLEX

By

Tamara Ann Reid

The kinematics of the shoulder complex were studied by non-invasive motion analysis and by developing a computer program which calculates the three-dimensional rotations of the shoulder . Because of the large range of motion at the shoulder, it was necessary to investigate and address several singularities. The mathematics used in the computer program created local coordinate systems on body segments and used Euler angles in the form of a joint coordinate system as introduced by Grood and Suntay (12) .

Six young men, who had no previous shoulder injury, performed a series of arm movements while 60 Hertz positional data were collected using a motion analysis system. The data were then read into the program and three angles were calculated: the internal/external rotation of the humerus, the rotation of the humerus in a transverse plane relative to the thorax and the elevation angle.

DEDICATION

I would like to dedicate this piece of work to my parents who have given me guidance and support (both morally and financially) throughout my entire life. Thank you for always being there for me.

To my husband, Neil, thank you for keeping me sane and for believing in me throughout this entire ordeal - I love you.

ACKNOWLEDGMENTS

The author would like to express her sincerest gratitude to the following people for their efforts, advice, and encouragement in the completion of this thesis.

To my co-workers and friends for their help and support: Gordie Alderink, Cheng Cao, Shawn Evans, Kathy Hillmer, Brock Horsley, David Marchinda, Jim Patton, Leann Slicer and Patricia Soutas-Little

I would like to extend special thanks to Yasin Dhaher for spending many hours with me both as a friend and as a colleague.

I would also like to thank Kim Lovasik for her everlasting friendship and support.

To my graduate committee: Dr. Robert Hubbard and Dr Dahsin for their friendship and for taking the time to review my work.

To my graduate advisor: Dr. Robert Soutas-Little we've spent much time together over the last four years, I've learned a great deal from you and would like to thank you for your guidance and friendship.

This is an accomplishment I am proud of and all of you helped make it possible. Thank You.

TABLE OF CONTENTS

LIST OF TABLES

LIST OF FIGURES

RESULTS:

INTRODUCTION

The shoulder complex has been stated as being the most difficult system of joints in the human body to kinematically evaluate (7). The reason is because it is a compilation of four articulations: acromioclavicular articulation , the scapulothoracic articulation, the sternoclavicular articulation and the glenohumeral joint (14, 5) (Figure 1). The sum of these articulations creates joints allow different ranges of movement; each articulation is not solely responsible for one type of motion, they all work together. To understand the shoulder complex and to define it clearly, it is necessary to elaborate on the four articulations. The acromioclavicular joint is the articulation between the acromial end of the clavicle and the acromion of the scapula. It is held together by various ligaments which run between the coracoid process of the scapula and the clavicle. This ligamentous connection gives the articulation a " joint" characteristic. Sometimes, this region is considered as two joints, the acromioclavicular and the coracoclavicular joints (5). The scapulothoracic articulation does not fit the typical hinge or ball and socket " joint" description either, but is a point at which the scapula rotates on the thorax. The sternoclavicular joint is the articulation between the sternal end of the clavicle and the sternum. This is described as a "saddle" type joint where the clavicle and sternum

Ventral or Anterior Aspect

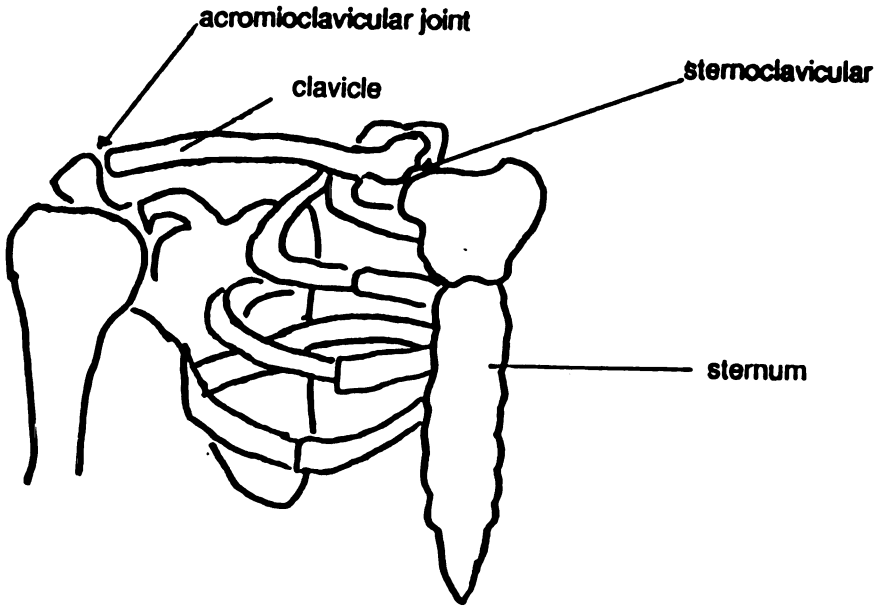

Dorsal or Posterior Aspect

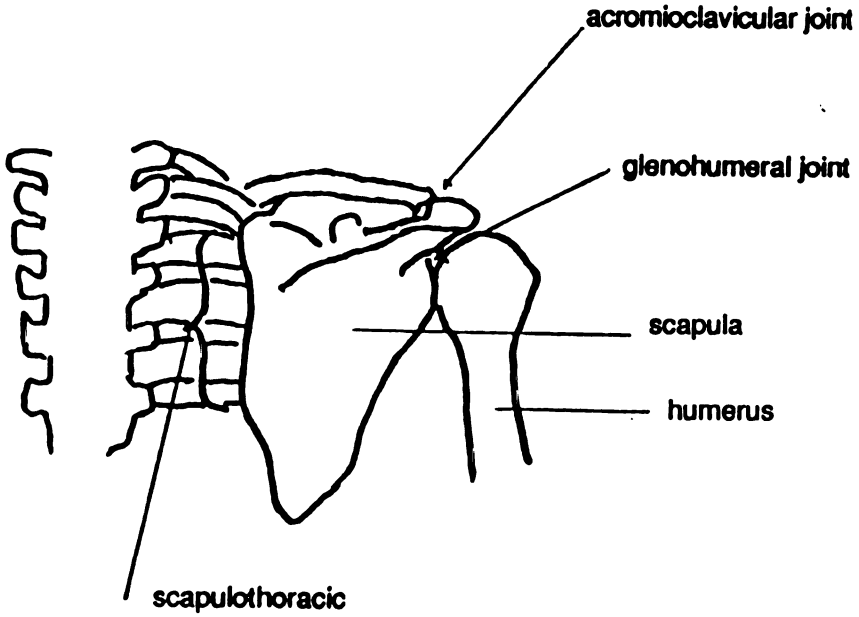

Figure1: Shoulder Articulations

are concave and convex surfaces, respectively, separated by a intraarticular meniscus, and the right and left sternal ends of the clavicle are connected by an interclavicular ligament. The glenohumeral joint is the joint which many people refer to as the shoulder. This is a ball and socket joint between the glenoid fossa of the scapula and the head of the humerus. (7,16)

Since the shoulder is extremely complicated, several methods of analysis have been studied. These methods include mathematical models which simulate the movement of the shoulder, cadaver experiments which deal with only the scapula, clavicle and humerus (1, 2, 5), cinematographic (19) and roentoeographic studies (13). Unfortunately, none of these are dynamic movement studies; therefore they are very difficult to apply to a clinical patient. One objective of this thesis is to develop a protocol which can be used easily and quickly for a clinical evaluation, such as a range of motion test or for sports enhancements such as baseball pitching.

A problem occurs in the method of defining the shoulder movements. The most popular method used by clinical individuals and sports biomechanists is to define the motions in three separate planes such as flexion/extension, abduction/adduction, and internal/external rotation. However, this becomes extremely confusing when a movement falls between two planes or when two or more movements are coupled. To further complicate matters, the order of motion is important as we find out by Codmans Paradox where an individual can perform two sets of movements and end in the same final position (Figure 2).

Rotation Set #1

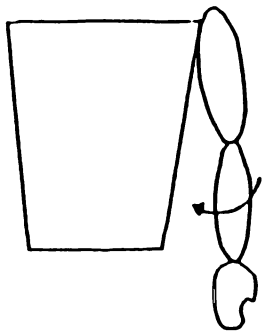

Anterior View

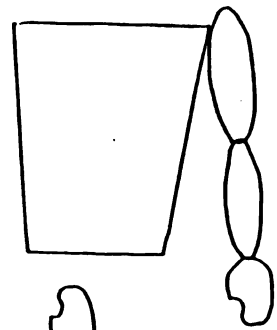

Rotate about the humerus 180°

Rotation Set #2

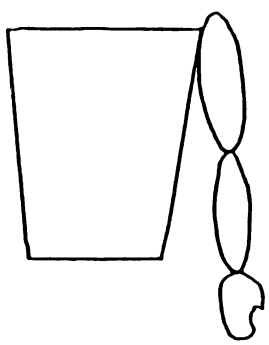

a.

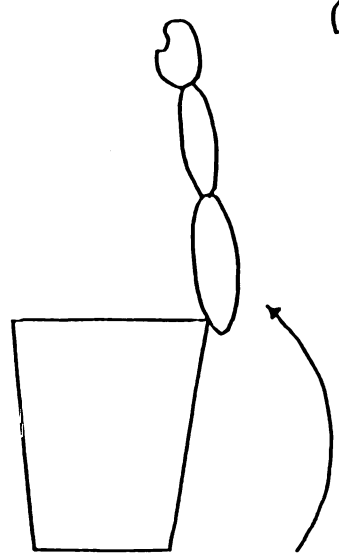

b. 180° Abduction

Side View

c. 180° Flexion

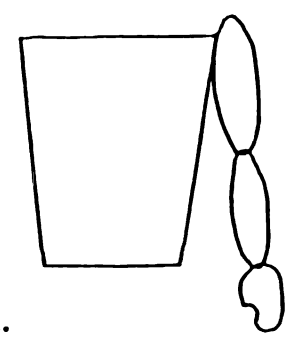

d.

Figure 2: Codman's Paradox

EXAMPLE:

First Rotation Set :

a. Start with the arm in the anatomical neutral position.

b. Rotate the arm 180^{o} along the humerus axis, now the palm is facing posteriorly.

Second Rotation Set:

a. Start with the arm in the anatomical neutral position.

b. Abduct the arm 180^{o} in the frontal plane.

c. Flex the arm 180^{o} in the sagittal plane.

After the second rotation set, the arm is at the side of the body with the palm facing posteriorly, yet axial rotation of the humerus did not occur (17).

One solution to the angle definition problem was proposed by An et al., at the Mayo Clinic (1). They chose to form an imaginary globe around the humeral head of cadavers (Figure 3). This type of descriptorhas also been termed globographic (7, 3, 5). An et al. (1) described the motion of the shoulder by an elevation angle (the latitude lines on the globe), a rotation in the elevation plane (the longitudinal lines) and internal/external rotation about an axis down the humerus (Figure 4). This naming convention eliminates the confusion of the separate plane description and with these three angles, the position of the humerus is uniquely defined.

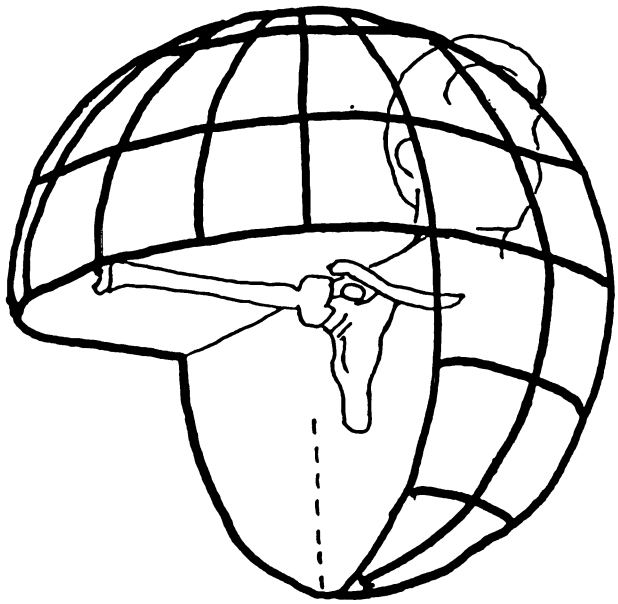

Figure 3: Globographic Representation

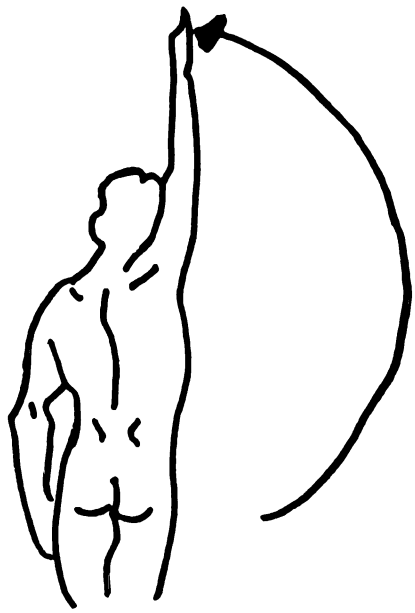

a. Elevation Angle

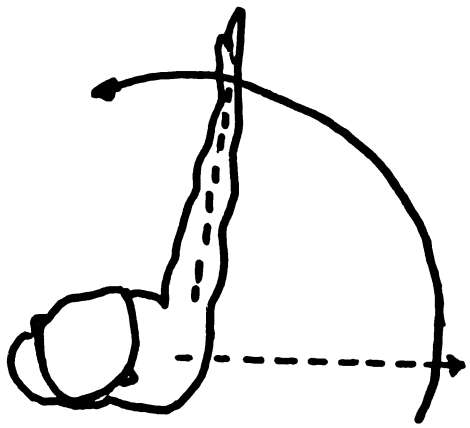

b. Rotation Plane Angle

Posterior Aspect

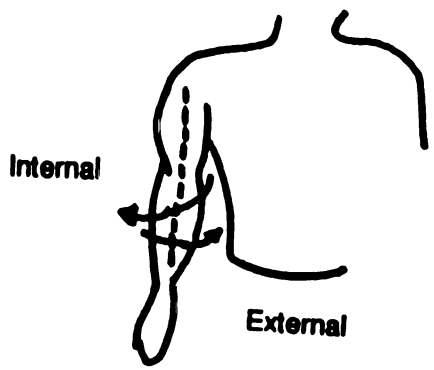

c. Internal and External Rotation

Figure 4: Shoulder Angle Description

Overall, the object of this thesis is to study the kinematics of the shoulder complex *in vivo*. This data will be calculated and presented in a similar fashion to the work presented by An et al..

LITERATURE REVIEW

Several methods of studying the shoulder complex have been used over the last century. Individuals began the analysis of the shoulder by studying the osteology, the musculature and the ligamentous structures of the shoulder complex (2, 5, 14). Dempster (5) and Inman (14) are known for pioneering studies on the shoulder.

Inman et al. (14) published a thorough article including an anatomical comparison analyzing the morphological changes of the scapula and humerus between several other species. He also used roentgenography and pin insertion to compile an analysis of the ranges of motion at the shoulder. From this data, Inman et al. set up equations to calculate the forces at the glenohumeral joint. To verify this data, he recorded the changing action potentials (electromyography) of ten different muscles. From their data collection on both cadavers and living subjects, Inman et al. formed the conclusion that, contrary to the teaching of that time period, the scapular and humeral motion are simultaneous, not successive. He also stated that, for free and full elevation, a lateral rotation of the humerus was necessary.

Dempster's study (5) broke the shoulder complex down into three distinct joints and then discussed the functionality and ranges of motion of each. He also discussed the role of associated ligaments and the restraining ability they have on the shoulder complex. In the" Mechanisms

of Shoulder Movement", Dempster separated the upper body into three links, the clavicular, scapular and humeral. His definition of a link is a straight line span between pivots at both ends of a bone. He treats the body as a mechanism and creates open and closed chain system of links. (Figure 5). From this method, Dempster looked at positions of the arm in three different planes, the transverse, frontal and sagittal (Figure 6). Internal and external rotation of the humerus were not examined. In this study, all data were collected from cadavers. Dempster also introduced the "joint sinus" which is described as the continuous boundary of a single joint's extreme range. Other authors have taken this idea and expanded on the notion (3, 8).

A third article entitled "Human Mechanics - Four Monographs Abridged" is a compilation of work from Braune, Fischer, Amar and Dempster (3). Some sections gave specific attention to the shoulder complex. The shoulder was discussed relative to kinematics and anthropometrics. These results were extracted from cadaveric data. In this pamphlet, the entire human body was discussed and the goal was to use the collected data to create a manakin which would adequately model a human. One diagram which confirms the point that the shoulder motion is a compilation of all four articulations, (acromioclavicular, sternoclavicular, scapulothoracic and glenohumeral) is shown in Figure 7. This diagram, produced from a cinefluorographic film, displays the path of the instantaneous center of rotation for one motion, abduction.

The above authors (3) also mention the globographic representation of kinematics of the shoulder and they note that " Simple globographic presentations used by others are inadequate for this joint due to lack of

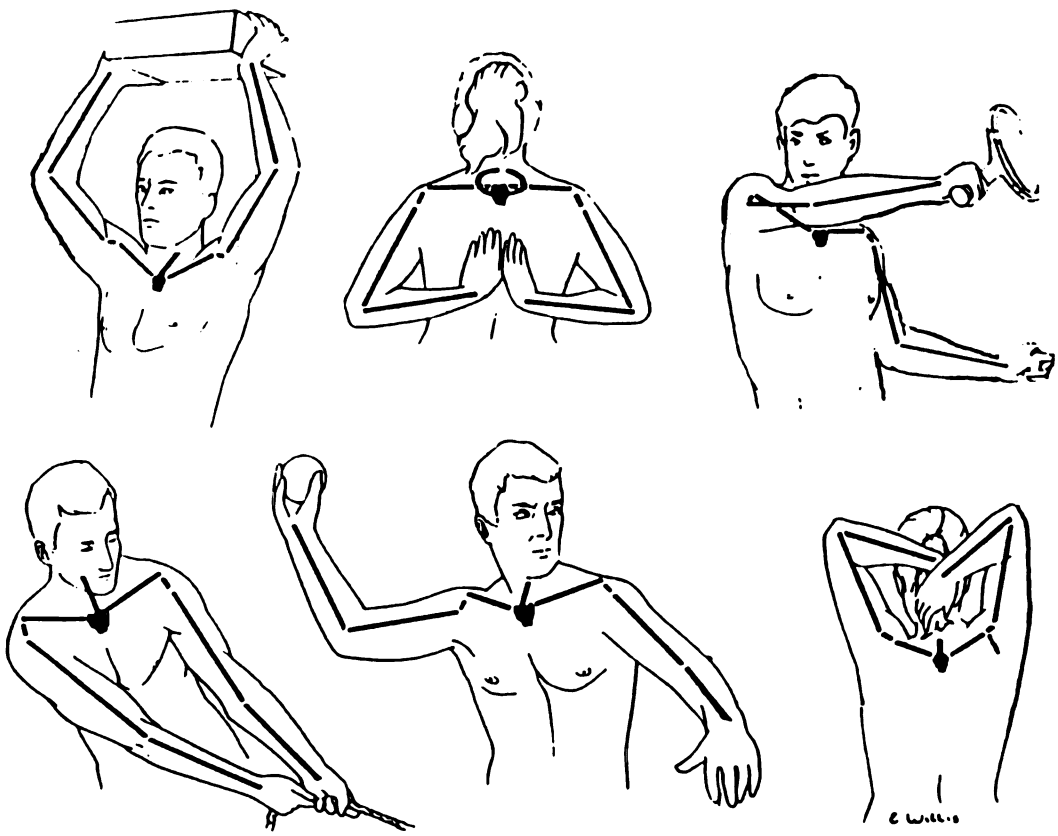

Various upper-limb postures with arm and forearm links, shoulder-girdle links, and sternocostal link (shown in two interpretations).

Figure: 5 Dempster's Linkage System

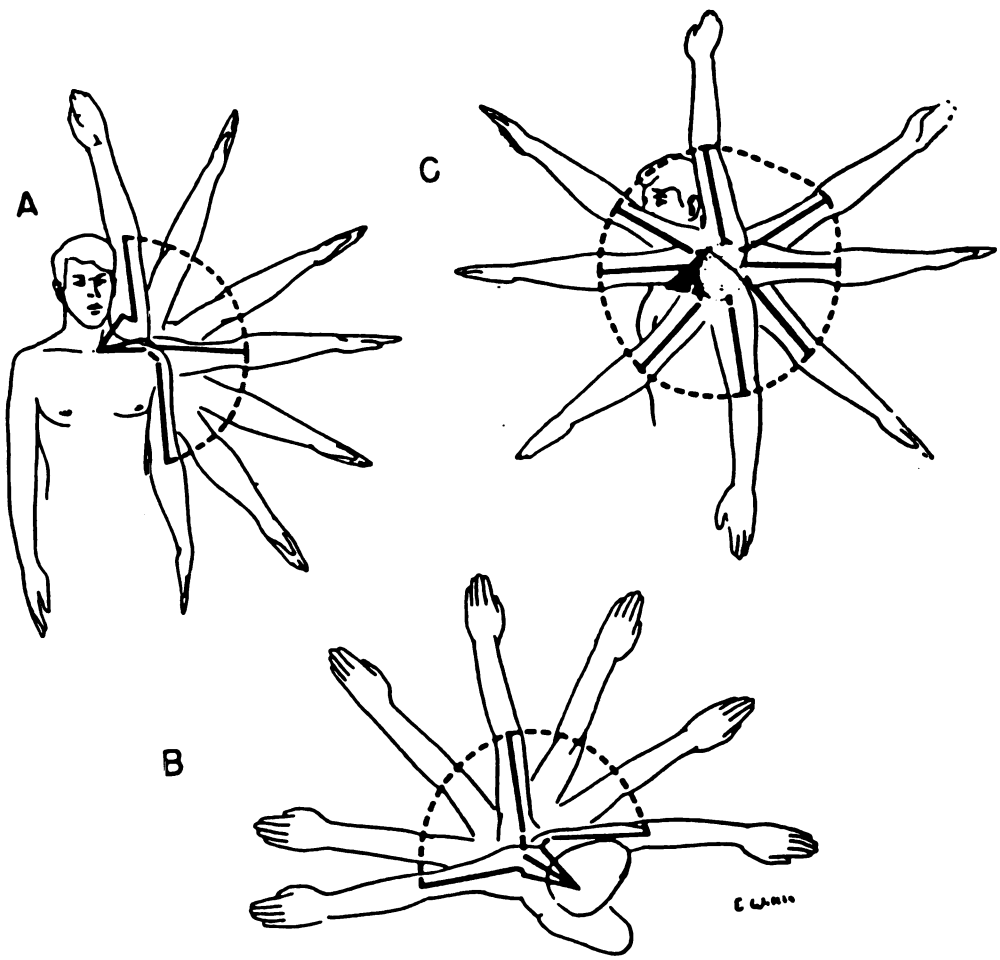

-Different positions of the upper limb and of the shoulder and arm links, in the plane defined by the scapula at rest. B—Positions of the limb and links in horizontal movement at shoulder height. C—Extreme positions of the upper limb; stippled cone represents the range of total clavicular motion. In each sketch, the line of dashes shows the elbow position.

Figure 6: Dempster's Planar Analysis

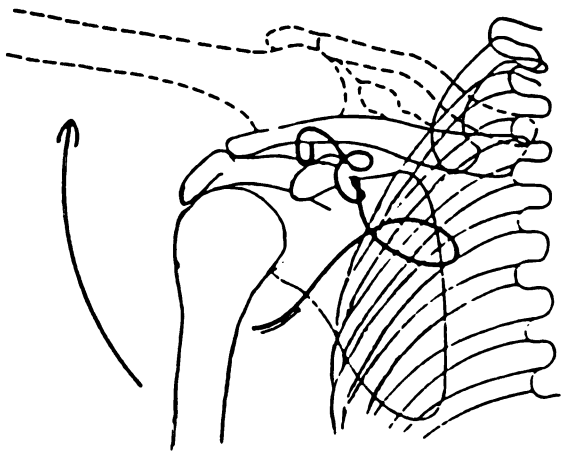

Path of Instantaneous Center of Rotation During Shoulder Abduction

Figure 7: Path of Instantaneous Center of Rotation

consistency in the locus of the center of rotation. However, they do represent gross values and have some value.".

Only for completeness of this thesis, the anthropometric data are presented in the form of tables. This data is shown in Table 1 (3).

The globographic method of describing the motion at the glenohumeral joint is not a new concept. Shino and Pfuhl (3) used this type of analysis in the early 1900's. Since then several biomechanists have adopted this method of analysis. Although this method does not have the capabilities of isolating the motion of each joint in the shoulder complex, it does allow for the tracking of relative motions between the thoracic cage and the humerus in a living subject. The simplicity of this descriptor is obvious when we look at what those in the clinical field are using to describe the motion at the shoulder.

The common clinical descriptions allow for little deviation and include flexion, extension, abduction, adduction and internal or external rotation (15). If the subject is not in one of these planes performing this exact motion, the system becomes complex and the descriptors become muddled and confusing. First, the planar definitions or common clinical descriptors will be discussed.

In 1959, the American Academy of Orthopedic Surgeons appointed a committee to study Joint Motion. This study was published as the Joint Motion Method of Measuring and Recording (15), and is the guideline for describing the motion which occurs at certain joints. It is necessary to understand the present method for description of joint motion in order to fully comprehend the simplicity of the globographic model and the three angles discussed in this thesis. During the time frame in which this committee assembled these guidelines, it should be noted that a

Table 1: Anthropometric Data

Joint and Type of Movement	Median (n=11)		Muscular (n=11)		Thin (n=10)		Rotund (n=7)	
WRIST:								
Flexion	94.6°	± 5.2	91.9°	± 9.4	95.6°	± 9.0	79.7°	±14.8
Extension	102.0°	± 8.9	97.0°	± 9.0	100.0°	± 8.3	86.8°	±17.8
	196.6°	±12.2	188.9°	±14.5	195.6°	±14.1	166.5°	±26.7
Abduction	25.1°	±10.2	27.1°	± 7.6	28.8°	± 7.9	27.5°	± 8.0
Adduction	46.3°	± 5.1	47.4°	± 6.4	47.1°	± 6.7	46.1°	± 6.4
	71.4°	±13.6	74.5°	±12.4	75.9°	± 9.8	73.6°	±12.9
FOREARM:								
Supination	100.6°	±22.1	113.3°	±15.8	123.8°	±20.0	114.8°	±19.2
Pronation	74.0°	±17.0	69.1°	±14.8	75.0°	±18.0	89.0°	±37.9
	174.6°	±26.0	182.4°	±18.6	198.8°	±22.9	203.8°	±42.3
ELBOW:								
Flexion	141.0°	± 9.8	140.3°	± 7.6	144.6°	±10.2	143.2°	± 8.6
SHOULDER:								
Flexion	193.2°	± 9.6	190.2°	± 9.9	186.0°	±11.7	184.0°	±12.2
Extension	63.0°	±14.3	58.1°	± 9.1	67.0°	±11.1	54.5°	±14.8
	256.2°	±17.7	248.3°	±10.3	253.0°	±17.3	238.5°	±23.9
Abduction	132.1°	±16.5	135.0°	±10.4	142.5°	±19.0	127.5°	±12.3
Adduction	50.8°	± 6.4	44.3°	± 6.7	53.5°	± 8.9	43.6°	± 5.2
	182.9°	±17.1	179.3°	±12.8	196.0°	±23.3	171.1°	±16.2
Medial Rotation	95.7°	±25.4	95.2°	±20.9	97.0°	±13.8	100.1°	±24.6
Laterial Rotation	30.7°	±13.1	33.0°	±13.7	39.5°	±10.1	32.5°	± 8.5
	126.4°	±24.4	128.2°	±28.5	136.5°	±16.7	132.6°	±15.6

globographic description of motion was proposed, but did not receive sufficient support. At the present time, biomechanists and clinicians are consolidating their research, methods and information in a call for standardization (4).

The following are some of the definitions given for shoulder motion with all references being relative to the anatomical neutral position:

I. Vertical or upward motion of the shoulder

Figure 8A. Abduction and Adduction

Abduction is the upward motion of the arm away from the side of the body in the coronal plane, from 0° to 180°. Adduction is the opposite motion of the arm toward the midline of the body, or beyond it in a upward plane.

Figure 8B. Forward Flexion or Forward Elevation and Backward Extension

Forward flexion is the forward upward motion of the arm in the anterior sagittal plane of the body from 0° to 180°. The opposite motion to the zero position may be termed depression of the arm. Backward extension is the upward motion of the arm in the posterior sagittal plane of the body from zero degrees to approximately 60 degrees.

II. Horizontal Motion of the Shoulder

Figure 8C Horizontal Flexion

Horizontal flexion is the motion of the arm in the horizontal plane anterior to the coronal (frontal) plane across the body. This motion is measured from zero degrees to approximately 130-135°.

Horizontal extension is the horizontal motion posterior to the coronal plane of the body. Figure 9 gives a description of the motion when the arm is in the horizontal plane (transverse plane). Descriptors become confusing when the arm is over the head, abducted and extended (Figure 10), the

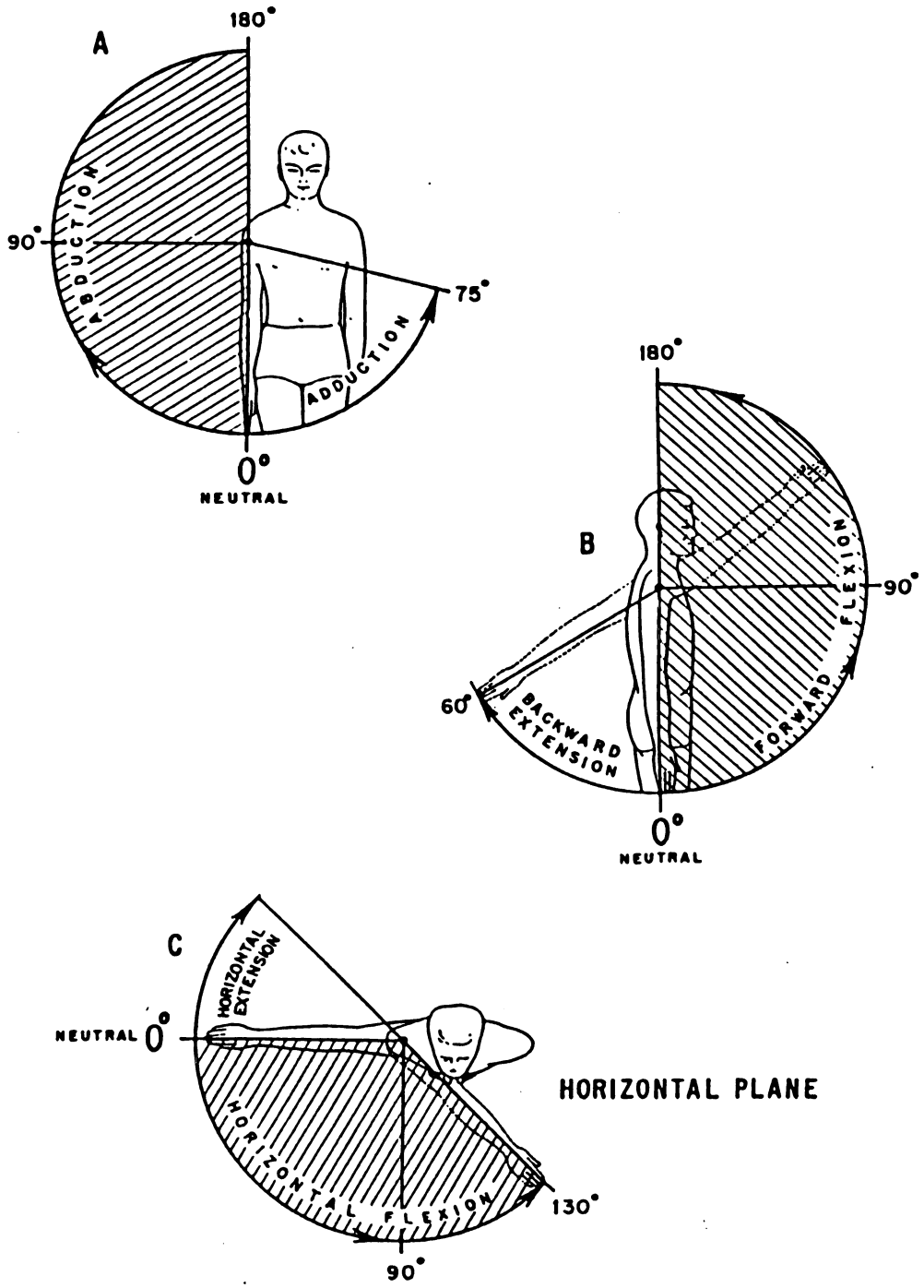

Figure 8: Planar Descriptors of Shoulder Motion

TERMINOLOGY IDENTIFYING UPWARD MOTION
OF THE ARM IN VARIOUS HORIZONTAL POSITIONS

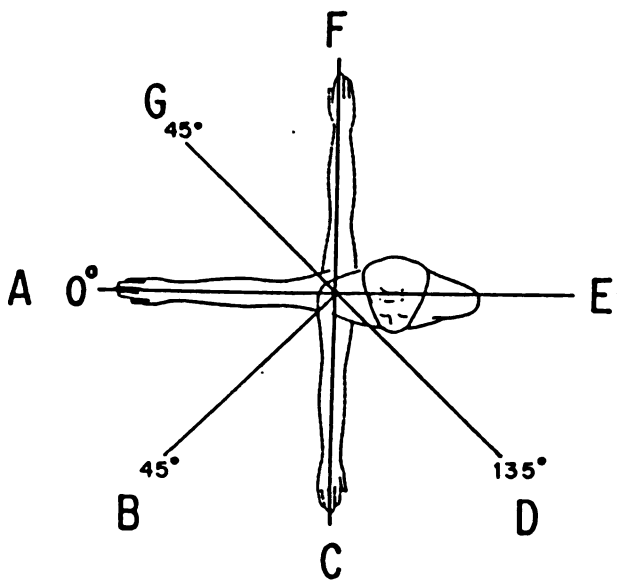

POSITION A = Neutral abduction
B = Abduction in 45° of horizontal flexion
C = Forward flexion
D = Adduction in 135° of horizontal flexion
E = Neutral adduction
F = Backward extension
G = Abduction in 45° of horizontal extension

Figure 9: Motion of Humerus in the Horizontal Plane

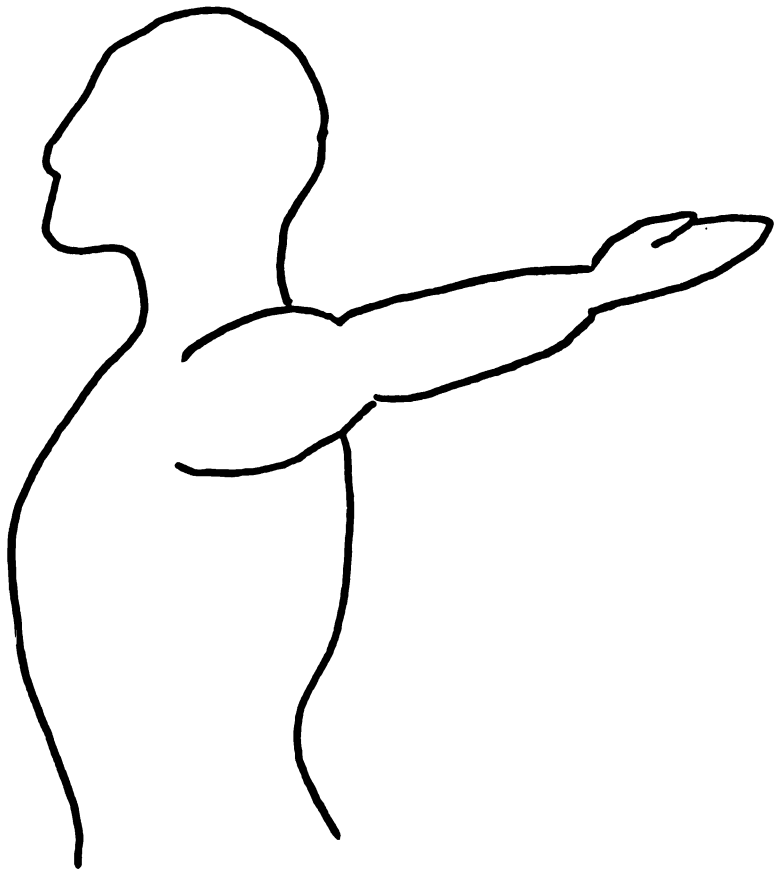

Sagittal View

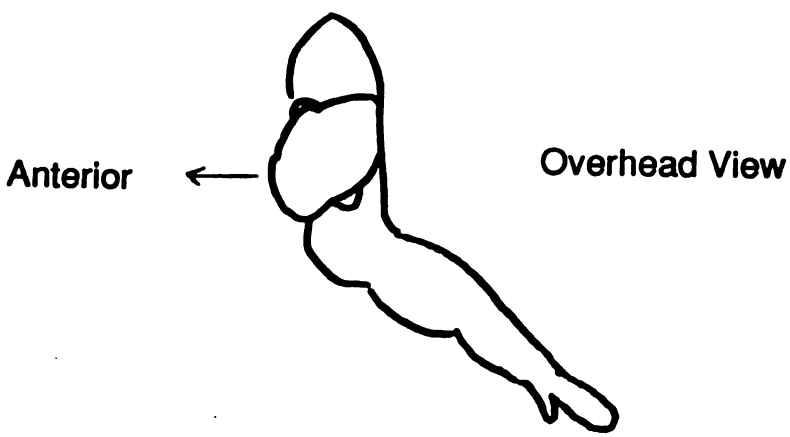

Figure 10: Non-Planar Motion

humerus is not longer in one defined plane.

The globographic system is useful, because as presented by Engin and Chen (8) and An et al. (1), this simplifies three dimensional data into two components, latitude and longitude. Combining this with the internal or external rotation of the humerus, the motion of the humerus relative to the thorax is uniquely defined.

Cinematographic (19), X-ray, roentgenographic, goniometry (7) multisegmented mathematical models (11), mechanism models (11), sonic digitizing (7) are among some of the other methods used to try to better understand the shoulder complex. Few individuals have analyzed dynamic motion of the shoulder complex. The *in vivo* methods reviewed have restrictions on the motion. The advantage to the type of analysis proposed in this thesis is that the subject is free to move in a natural sense, and because this form of motion analysis is non invasive, these are the true recordings of the subject; in other words, is no artifact is introduced because of pain caused by a brace or pin insertion.

Several other scientists have investigated the kinematics of the shoulder complex. Engin (7), in one of his experiments collected resistive force, moment and torque data on living subjects. Engin developed an exoskeletal device(ESD)) and a global force applicator (GFA). The exoskeleton device is a measuring instrument which is fitted to the arm on bony landmarks and allows freedom of motion between the arm and torso. The GFA moved the arm through a certain range of motion applying a specific amount of force while the subject sat in a restraint system.

Engen (10) used three mirrors and a 35mm camera to compare the motion of an anatomical arm to a motorized arm. He had the subject perform tasks such as hair grooming, writing, page turning and table to

mouth feeding. He used time clocks to calculate the velocity and acceleration of points on the arm.

Engin and Chen (8) used sonic emitters to track the motion of the humerus relative to a fixed torso. They used 10 subjects in the age range between 18 and 32. Three sonic emitters on each body segment were used to create a joint coordinate system on the humerus and the torso. During data collection, the torso was immobilized while the subject moved the arm in a maximum range. The data was then displayed in a globographic representation. Once again, the body was not free to move in a natural sense because of the thorax immobilization.

Hogfors et al. (13) performed an experiment in which the arm and torso were uninhibited by any sort of brace or mechanism but the movement was limited by the size of film. His group inserted radiation dense implants into the shoulder region and monitored the motion by roentgenstereophogrammetry. Four tantalum balls were inserted into each of the following three spots: proximal humerus, lateral acromion and lateral clavicle. He had the subjects perform "spiral arm lifts" with 1 and 2kg weights. He then calculated the motion by using the Z, Y', X" order of Euler angles (Figure 11). This data analysis does not limit the motion of the subject, however it is not feasible to insert radiation dense balls into every subject.

Lastly, An et al. (1) using a magnetic tracking system studied three-dimensional glenohumeral joint motion in cadavers during arm elevation. He used a Z X' Z" order of Euler angles to evaluate the tracked data and the globographic representation of the data. He noted that there would be singularities in the analysis if the elevation of the arm reached 0° or 180° and only evaluated cadaveric data so these singularities could be

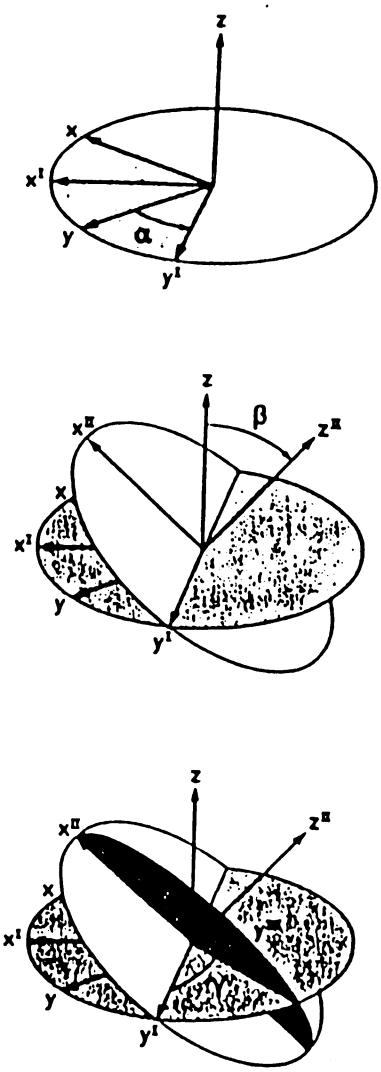

Figure 11: Cardan Angles

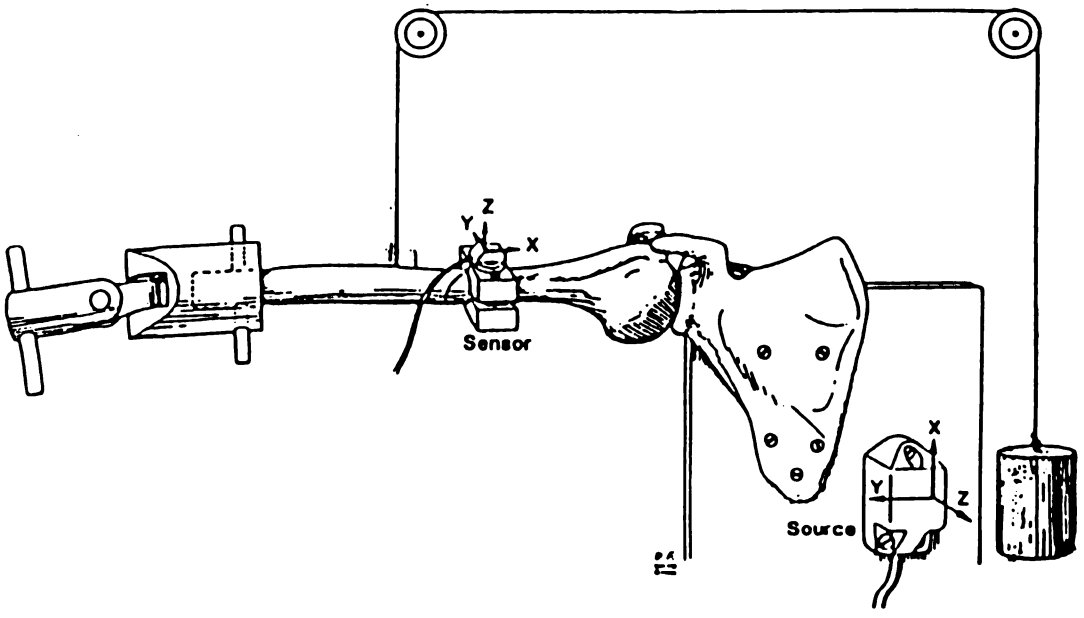

Figure 12: An et al. Experimental Setup

avoided (Figure 12). An et al. (1), held the humerus at either a maximum internal rotation or a maximum external rotation, and were able to monitor the rotation of the humerus.

Methodology for a clinical analysisof shoulder motions has not been the subject of many investigations by the biomechanics community. The articles reviewed above are not concerned with identifying basic shoulder function and dysfunction. The objectives have been to anatomically identify the mechanisms in the shoulder. Much cadaveric data has been collected but it has been primarily used to created lifelike models. The *in vivo* kinematic data which has been collected in other studies has drawbacks when applied to the clinical setting, such as being invasive, limited by size of X-ray film or requiring one body segment to remain fixed.

EXPERIMENTAL METHODS

Before testing began, a calibration space was defined as a 1.5 m cube, beginning 70 centimeters from the floor. The square space was marked with four calibration stands (one on each corner). Each calibration structure consisted of four targets which when placed in the square arrangement created a box defined by 16 targets (Figure 13). For calibration, the largest targets (approximately 36mm in diameter) were used on the calibration structure. The targets were spherical and were covered in retro-reflective tape manufactured by 3M. The reflectivity of the tape is from 600 to 1600 times brighter than a white surface and has the highest amount of luminance at a 35° entrance angle (the angle between the light ray and the normal to the surface). The tape allows for a range of up to 60° for an entrance angle (18). Since the targets were spherical and there were four cameras with light sources, this entrance angle requirement was easily met. Once the calibration stands were in position, the four 60 Hz NEC shuttered video cameras were placed around the calibration space so they would provide optimum viewing of the subject. A light source was mounted approximately five centimeters to the left of the center of the camera lens. This light served as the lumination source for the targets and the threshold of these lights was adjustable on the

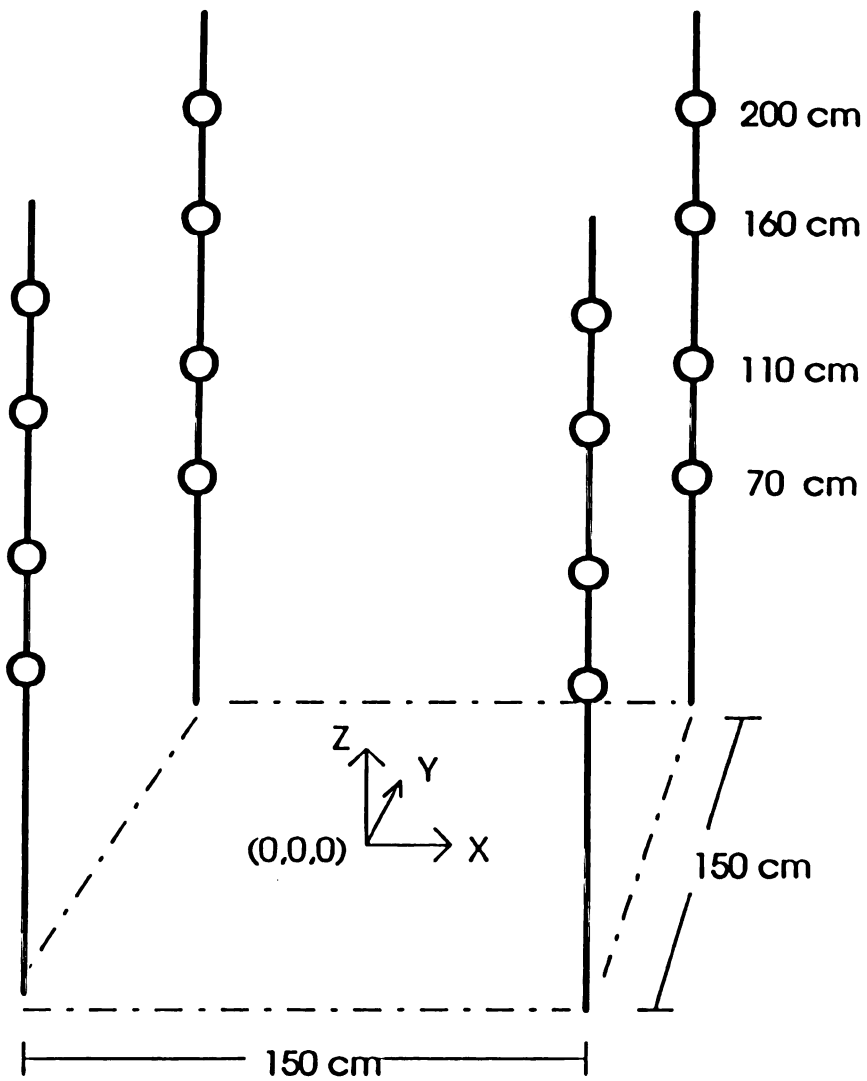

Figure 13: Calibration Structure

video processor (VP320 by Motion Analysis) to compensate for variations in light intensities.

Once the calibration space was set and the cameras were in position, data were collected for six seconds on marker positions in the calibration space. Data from the four cameras were sent through the VP320 which synchronized the four cameras. The dimensions of the calibration space were manually entered into the computer and then data were digitized in pixel space by the VP320 in real time. With the pixel coordinates and with the manually inputted laboratory coordinates of each target, transformation matricies were formed. This set of matrices allowed the data to be converted from lab space to pixel space by the method of direct linear transformation. The transpose of these matrices allowed the conversion from pixel space to lab space. These matrices were then stored in an environment file and were applied to the test data. The six seconds of digitized data then became the video file.

The accuracy was measured by a "norm of residuals". This was a number which related, for each camera, the least square solution of the transformation. For the shoulder evalution calibratiion, the norm of residuals were .31-.40 for the first day and .27-.59 for the second day. The residuals computed on day two were not as tight as day one, but due to multiple tests and time constraints on the subjects, this test space was used. These values were well below the system's value for the maximum norm of residuals and no tracking problems were encountered due to the larger span of residuals.

The subjects were six male high school baseball pitchers who had no previous shoulder injuries or surgeries. An informed consent was sent to each of them, along with a consent form allowing photographic pictures

and video taping. All subjects brought their signed consent forms with them to the laboratory. All lab testing was done under # IRB89-559 approval. Prior to testing these anthropometric measurements were recorded for each subject:

1) Weight
2) Height
3) Hand Length from top of the wrist to the tip of the middle finger
4) Arm length from acromion process to the wrist joint
5) Shoulder breadth (which was measured as the width between the left and right acromion processes)

These measurements were not used in this study, but were obtained for future studies and reference.

After these measurements were obtained, each person was targetted. The spherical targets used were approximately 24 mm in diameter and were covered with the 3M retro-reflective tape, the same tape used in the calibration. Targets were placed on the following locations:

1) Medial Elbow Epicondyle
2) Lateral Elbow Epicondyle
3) Humeral Head
4) Sternal Notch
5) First Thoracic Vertabrae
6) Eighth Thoracic Vertebrae
7) Xyphoid Process
8) Medial Wrist
9) Lateral Wrist

The last three targets were not used in calculations, but were placed on the subjects to aid in tracking (Figure 14 and Figure 15).

The subjects were given a brief explaination along with a demonstration on what types of motions were desired. The subject initially began with their body erect and in the anatomical neutral position. While in the neutral position, a six second standing file was shot. All subjects began

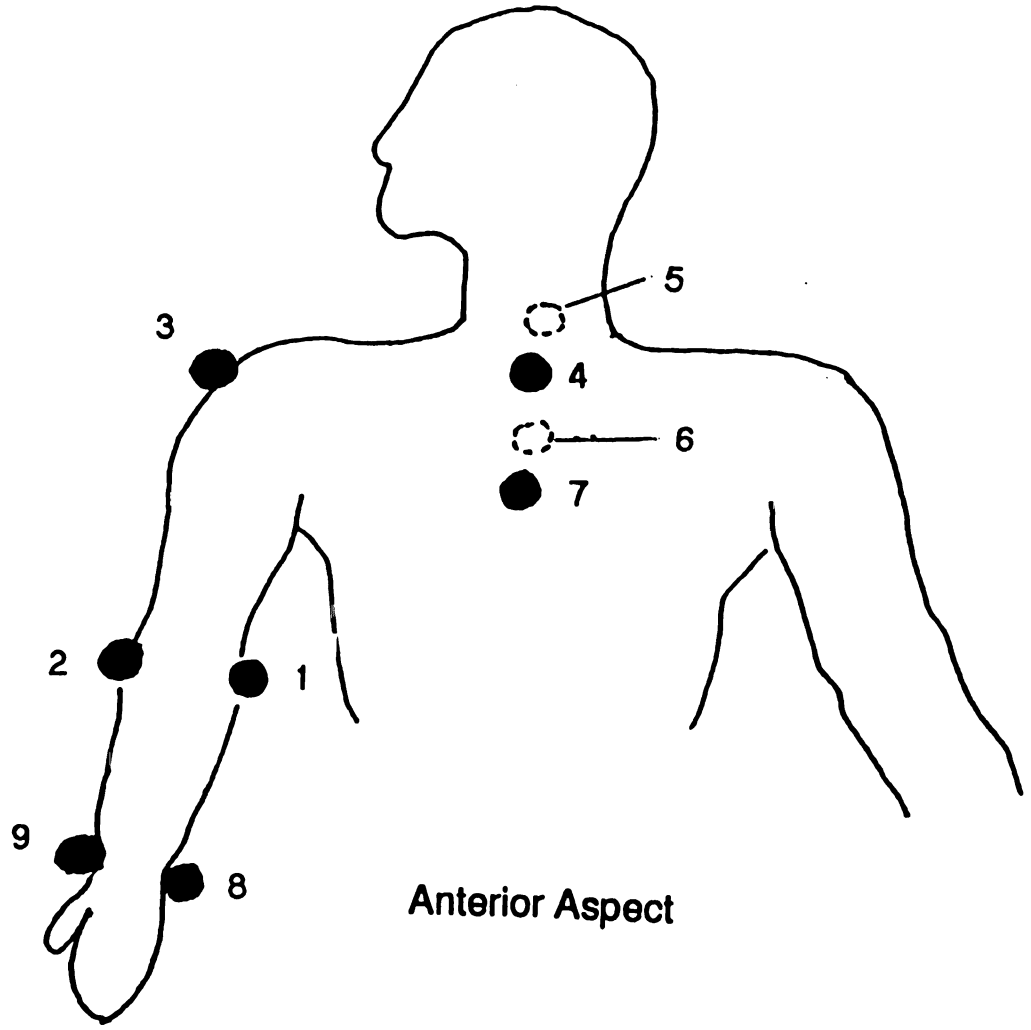

1) Medial Elbow Epicondyle
2) Lateral Elbow Epicondyle
3) Humeral Head
4) Sternal notch
5) First Thoracic Vertabrae
6) Seventh Thoracic Vertebrae
7) Xyphoid Process
8) Medial wrist
9) Lateral Wrist

Figure 14: Frontal View of Targets

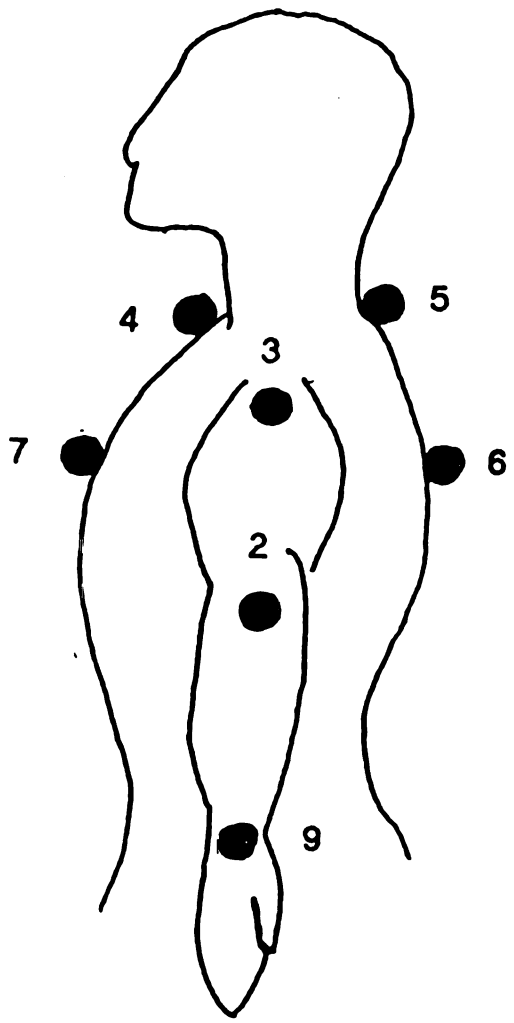

Figure 15: Sagittal View of Targets

each trial in the anatomically neutral position and after a cue was given, they moved into one of the three positions: arm internally rotated, externally rotated or in a relaxed position and then they began their range of motion movement. The subjects were asked to hold their arm in the desired position as "best able" throughout the trial. The relaxed position began with the arm in the neurtal position and then on the cue, they internally rotated their arm until the thumb was pointing anteriorly. They then began the movement allowing their arm to rotate comfortably in order to achieve the maximum range of motion at the shoulder.

Each subject had a series of ten trials:

1 neutral
3 internally rotated
3 externally rotated
3 in relaxed position

Each trial was 10 seconds in duration. The path which the individual followed in order to obtain maximum range of rotation at the glenohumeral joint is described in the following paragraph.

RANGE OF ROTATION:

After the subject first rotated the humerus to one of the three specified conditions (internal,external or relaxed) (Figure 16a), the movement of the arm began posteriorly (Figure 16b). The subject first extended his arm posterior to the thorax then while moving posteriorly and elevating the arm he brought it as close to the midline of the thorax as possible (Figure 16c). The subject then raised the arm superiorly behind the back and eventually over his head. (Figure 16d) The arm was lowered down and across the front of the body (Figure 16e & f), then back to the starting region (Figure 16g). The subject was asked to continue for ten seconds.

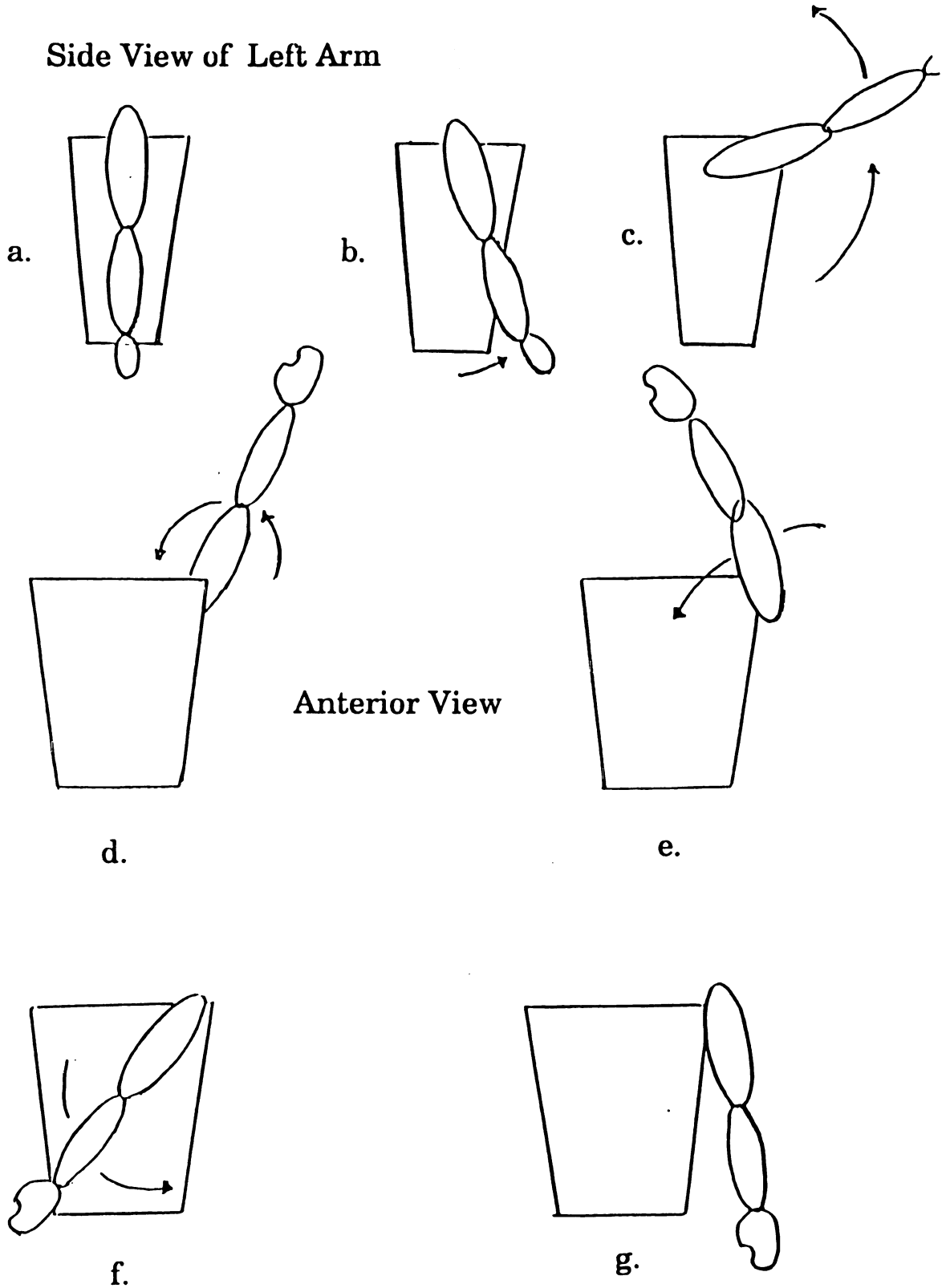

Figure 16: Range of Rotation

Most subjects achieved two full rotations. The object of this movement was to obtain the largest range of motion at the glenohumeral joint.

All subjects were photographed with a polaroid camera while in the anatomically neutral position. Subjects were also photographed with a 35mm camera at random positions while performing the series of tests. All trials of each subject were also videotaped using a Sony camcorder.

ANALYTICAL METHODS

After the data were collected, the raw video files were first viewed and frames of merged targets were identified. After identification, a mask operator in the ev3d software was used to separate the merged targets, one pixel at a time. The mask operator acted like an editor for the motion files; this allowed the user to delete an entire target or just a few pixels. Each camera's data was analyzed individually.

Separating the merged targets slightly decreased the accuracy of identifying the centroid of the target, although it was felt that having a fragment of an actual target was better then joining over a merged area where the target position would have been eliminated completely. A merged target occurs when the view from a camera identifies two targets as having centroid locations which are extremely close. The targets appear to come together and form one large target. This commonly happened with the elbow targets.

After the files were masked, they were tracked using the ev3d software by Motion Analysis. This system tracks all four cameras simultaneously in three dimensions and was described in detail in the Experimental Methods section. If a target was obscured and the target could not be identified in two cameras, the computer could not triangulate on the target and therefore, could not determine its location. Thus, the

trajectory of that target was incomplete and interpolating in the trajectory path could not be avoided. The interpolation fit a cubic spline between the tracked trajectory segments. Great care was taken to assure the best possible fit and any inconsistent trials were discarded.

The kinematic data was smoothed by digital filtering which was done before the angles were calculated from the tracked data. A tracked file appears in Figure 17.

Data were mapped into a position format where one time was given and all target positions were listed below that time. The data were then run through the shoulder angle program developed for this thesis. This program gave the position of the humerus relative to the thorax by using the previously described system: an elevation angle, a plane of rotation and internal/external rotation of the humerus.

A local coordinate system was developed on each segment by using the three targets placed on that segment. Two of the targets on the body segment always identified an anatomical axis, while all three identified an anatomical plane. On the thorax, the two vertebral targets defined the superior/inferior anatomical axis and the sternal notch target , along with the two vertebral targets defined a sagittal plane. The two vertebral targets were used to form the anatomical axis instead of the sternal notch and the base of the sternum targets because a universal targeting scheme was desired. On some individuals, particularly females, the sternum region might be a difficult and a sensitive area to target.

On the humerus, the lateral elbow epicondyle target and the humeral head target formed the anatomical axis while the medial elbow epicondyle target formed a frontal plane when the body was in the anatomical position.

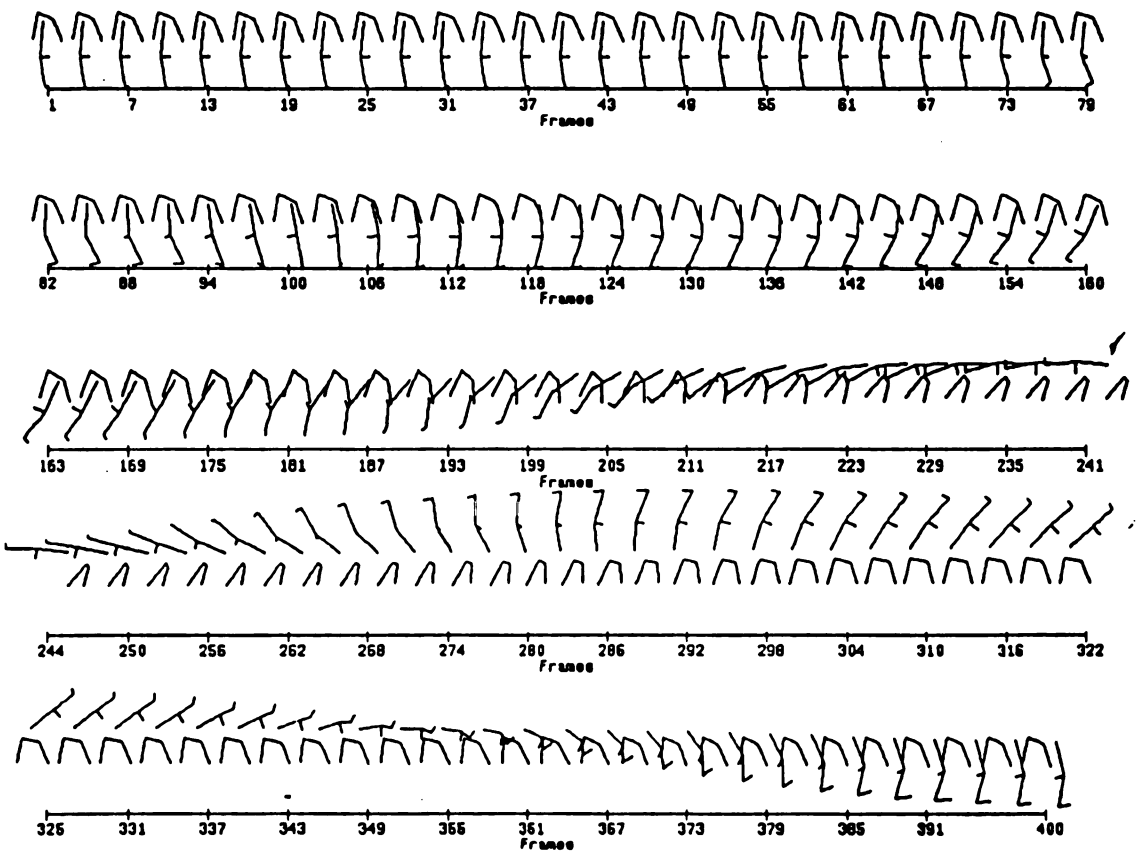

Figure 17: Tracked Stick Figure

The local coordinate system was formed on the thorax by identifying a vector from the eighth thoracic vertebrae to the first thoracic vertebrae as the Z_t axis of the thorax. A vector (G_t) was then formed from the first thoracic vertebrae to the sternal notch. The superior Z_t axis was crossed (vector cross multiplication) into the other axis formed between the sternal notch and the first vertebrae to obtain the Y_t axis which was defined as always pointing to the left:

$$Z_t \times G_t = Y_t$$

After each axis was created on each segment, each axis was made into a unit vector. This was done by taking each component of the vector and dividing it by the magnitude of that vector.

Magnitude: $M = \sqrt{x^2 + y^2 + z^2}$

Unit Vector: $\hat{U} = \frac{x}{M}, \frac{y}{M}, \frac{z}{M}$

Thus, Y_t was made into a unit vector where Y_t is the vector in terms of individual components and $|Y_t|$ is the magnitude :

$$\hat{Y}_t = \frac{Y_t}{|Y_t|}$$

The third axis was obtained by crossing the Y_t into the Z_t to obtain the X_t axis. The X_t axis pointed anterior (Figure 18).

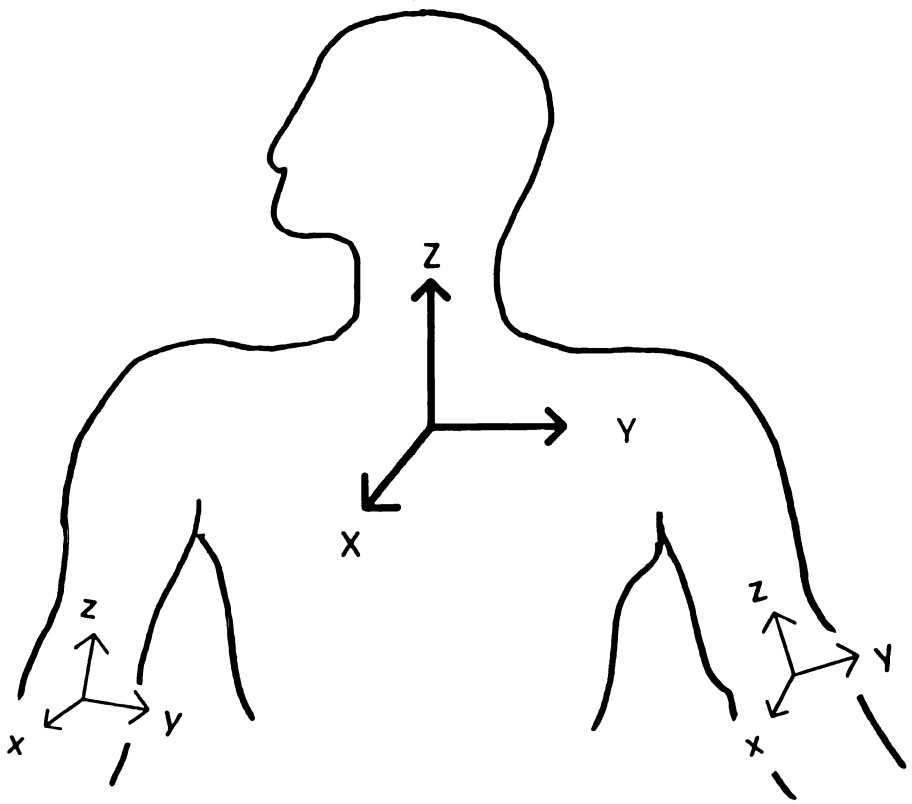

Figure 18: Segmental Axes System

$$Y_t \times Z_t = X_t$$

$$\hat{X}_t = \frac{X_t}{|X_t|}$$

Z_t was also made a unit vector:

$$\hat{Z}_t = \frac{Z_t}{|Z_t|}$$

Complications:

Since the targets that identified the thoracic Z axis were along the thoracic vertebrae, a natural kyphotic curvature existed between the location of the first thoracic vertebrae and the eighth thoracic vertebrae. This caused an initial tilt in the thoracic coordinate system which ranged from 8 to 20 degrees relative to the vertical of the laboratory space. When the arm is in the starting position (at the side of the body) the Z axis of the arm and the Z axis of the thorax are both in a vertical position and because these two axes are close to parallel, the cross-product used to define the floating axis is sensitive to small angle errors.

This initial tilt caused the position of the floating axis to be pointed medially and posteriorly for the time period the arm was at the side of the body. The vectors that form the floating axis were chosen under the assumption that, when crossed while the body was in the neutral position, the floating axis would be pointing anteriorly. Thus, the zero degrees of rotation in the elevated plane was chosen to be in line with the X axis of the thoracic cage.

In some cases, the Z axes crossed over each other and changed the position of the floating axis by approximately 180° , causing a discontinuity in the data. Once the thoracic coordinate system was aligned with the laboratory coordinate system, this problem was solved.

Adjustment to Lab Space:

To remedy the initial tilt due to the curvature of the back, the orientation of the thoracic coordinate system was recorded for the first frame of data and a transformation matrix was identified as:

$$[B] = \begin{bmatrix} i_{xx}, i_{xy}, i_{xz} \\ i_{yx}, i_{yy}, i_{yz} \\ i_{zx}, i_{zy}, i_{zz} \end{bmatrix}$$

where

$$\hat{X}_t = i_{xx}, i_{xy}, i_{xz}$$

$$\hat{Y}_t = i_{yx}, i_{yy}, i_{yz}$$

$$\hat{Z}_t = i_{zx}, i_{zy}, i_{zz}$$

which are the three components of each unit vector of the thoracic coordinate system relative to the lab coordinate system.

Next, the transpose of this matrix was identified as:

$$[B]^T = \begin{bmatrix} i_{xx}, i_{yx}, i_{zx} \\ i_{xy}, i_{yy}, i_{zy} \\ i_{xz}, i_{yz}, i_{zz} \end{bmatrix}$$

The transpose matrix of a rotation matrix is the inverse of the matrix. This is a unique characteristic only true to an orthogonal rotation matrices.

For the initial frame, the thoracic rotational matrix was multiplied by its transpose matrix. Visually, the matrix $[B]$ is the amount the initial thoracic coordinate system is rotated relative to the laboratory coordinate system and when multiplied by the transpose, the coordinate system is rotated back that initial amount, aligning the thoracic coordinate system with the laboratory system.

$$[I] = [B]^T [B]$$

$$[I] = \begin{bmatrix} 1, 0, 0 \\ 0, 1, 0 \\ 0, 0, 1 \end{bmatrix}$$

This action results in the identity matrix, which means the thoracic coordinate system and the laboratory coordinate system are aligned.

For each of the following frames, this same transformation matrix was used to rotate the thoracic coordinate system back this initial amount. The data was only normalized to standing data. A new transformation matrix was not computed for each frame, and if the thorax was rotated

medially of laterally during the course of the actual arm movement it was incorporated into the data analysis.

The local coordinate system was formed on the humerus by defining the segmental Z_h axis to be pointing superiorly when in the neutral position from the lateral elbow epicondyles toward the humeral head.

A vector was then formed from the lateral elbow epicondyle to the medial elbow epicondyle on the left side (G_h). On the right side, these same two targets were used to form this vector, but it was defined in the opposite direction. Then, the epicondyle vector was crossed into the Z_h axis to define the anterior/posterior axis of the humerus.

$$G_h \times Z_h = X_h$$

This was then made into a unit vector:

$$\hat{X}_h = \frac{X_h}{|X_h|}$$

The Z_h axis was crossed into the X_h axis to obtain the Y_h axis or medial/lateral axis and it was made into a unit vector (Figure 18).

$$Z_h \times X_h = Y_h$$

$$\hat{Y}_h = \frac{Y_h}{|Y_h|}$$

Lastly, Zh vector was also made into a unit vector:

$$\hat{Z}_h = \frac{Z_h}{|Z_h|}$$

Using Euler's angles with a Z X' Z" rotation and the method described by Grood and Suntay(12), joint coordinate systems were formed on each body segment and the three angles were computed.

The Euler angles represent three ordered rotational transformations. Euler angles may be formed in the following fashion. The first rotation which defines the rotation in the elevated plane is a rotation about the Z_t axis:

$$\begin{bmatrix} \cos\phi & \sin\phi & 0 \\ -\sin\phi & \cos\phi & 0 \\ 0 & 0 & 1 \end{bmatrix}$$

The second rotation defines the angle of elevation which is the rotation about the X' axis and is denoted as Euler's line of nodes or the floating axis as described by Grood and Suntay.

$$\begin{bmatrix} 1 & 0 & 0 \\ 0 & \cos\theta & \sin\theta \\ 0 & -\sin\theta & \cos\theta \end{bmatrix}$$

The third rotation is a rotation about the new Z" axis which is Z_h (Z of the humerus)and defines internal/external rotation about the humerus (Figure 19).

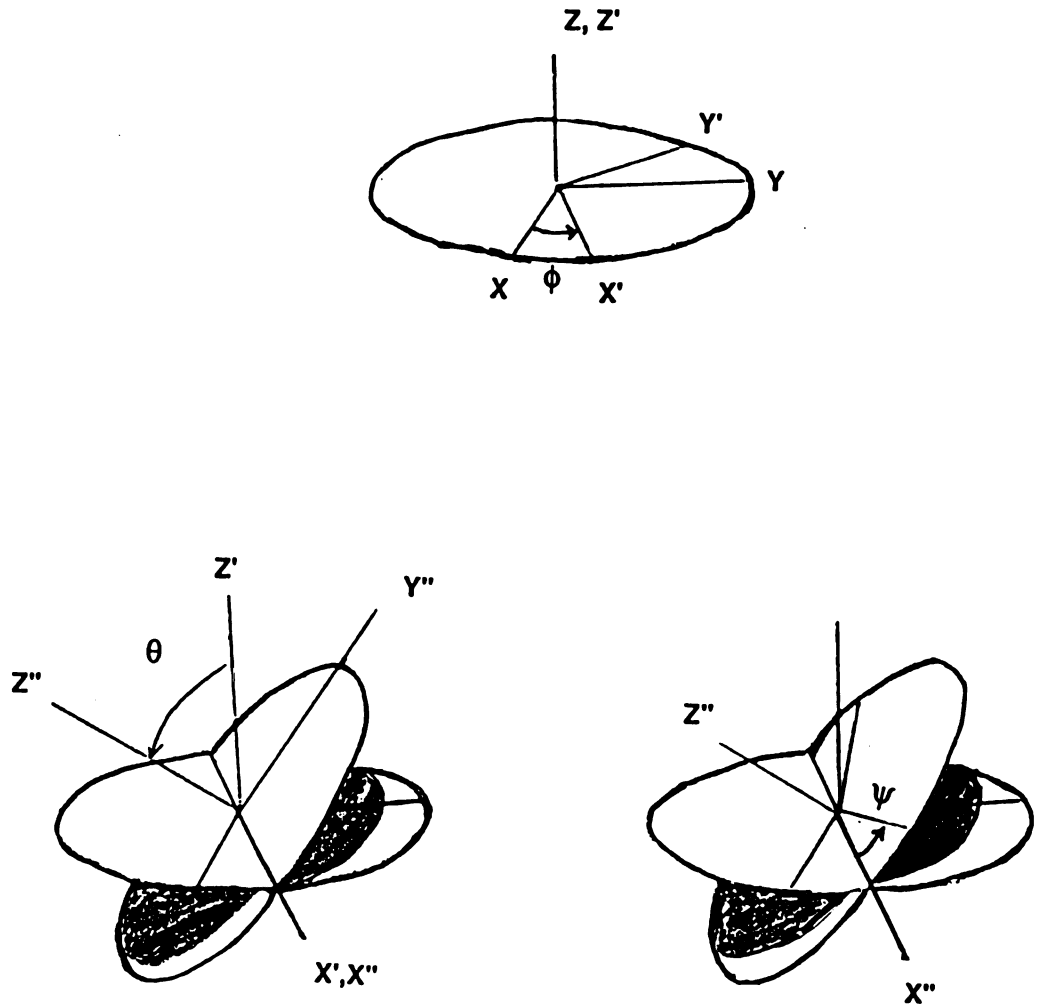

Figure 19: Rotation Z X' Z"

$$\begin{bmatrix} \cos\psi & \sin\psi & 0 \\ -\sin\psi & \cos\psi & 0 \\ 0 & 0 & 1 \end{bmatrix}$$

Obtaining the Euler angles in the above fashion requires that the three matricies be multiplied together and the angles be teased from this large and usually complex matrix. By using the analysis method of Grood and Suntay (12), the exact same angles can be obtained by using simple dot products. Thus the angles ϕ, θ and ψ can also be obtained as follows:

$\hat{e}_1 = \hat{Z}_t$ where $\hat{e}_1$ is the axis of rotation in the elevated plane

$\hat{e}_3 = \hat{Z}_h$ where $\hat{e}_3$ is the axis which internal and external rotation of the humerus occurs

$$\hat{e}_2 = \frac{\hat{e}_1 \times \hat{e}_3}{|\hat{e}_1 \times \hat{e}_3|} \text{ on the left side}$$

$$\hat{e}_2 = \frac{\hat{e}_3 \times \hat{e}_1}{|\hat{e}_3 \times \hat{e}_1|} \text{ on the right side}$$

where $\hat{e}_2$ is the floating axis or the line of nodes which is perpendicular to both $\hat{e}_1$ and $\hat{e}_3$ and is the axis of elevation.

These three unit vectors, $\hat{e}_1, \hat{e}_2, \hat{e}_3$, form a non-orthogonal joint coordinate system. It should also be noted that the switch of the cross product order from the left side to the right side was done to maintain the condition that the floating axis begin pointing anterior to the thorax. If this condition is met, then a sign consistency can be maintained between the right and left sides.

As put by Cole et al.(4), the method used by Grood and Suntay eliminates the sequence dependency by predefining the axes of rotation.

However a sequence effect is still imposed in the manner that one must decide upon the fixed body axes.

Calculation of angles and rotations:

** Note: from this point on, all vectors referenced in the text are unit vectors.

Elevation:

The elevation angle (Figure 20) was calculated by :

elevang = arccos $(\hat{Z}_t \bullet \hat{Z}_h)$ for angles greater than 10°

for angles less than 10°

elevang = theta

Theta was used to calculate the elevation angle for small values because using the arccos of Z_t dotted with Z_h is more likely to produce errors as the angle approaches zero. Looking at the cosine value for different angles, it can be seen that at the smaller angles, the sensitivity of the calculation is decreased, meaning that a slight difference in the cosine can make a large difference in the angle. For example between 0 and 15 degrees, the cosine ranges from 1 to .9659 which is only a difference of .0341 where the same 15 degree range taken from 70 to 85 degrees has a cosine range from .3420 to .0871, a difference of .2549. Thus to avoid some of the possible error in this region, the other two shperical angles, alpha and beta were found and using the relationship that $\cos^2\alpha+\cos^2\beta+\cos^2\theta=1$ the angle theta, which is the angle of elevation, was calculated.

The elevation angle did not reach 180° with any of the subjects so possible problems at the upper end did not have to be addressed.

Spherical angle calculations:

$$\text{alpha} = \text{acos}\ (\hat{e}_2 \bullet \hat{Z}_h)$$

$$\text{beta} = \text{acos}\ (\hat{e}_2 \bullet \hat{Z}_h)$$

$$\text{theta} = \sqrt{1.0 - alpha^{\,2} - beta^{\,2}}$$

Conceptually, this is the angle between the humerus and the superior axis of the thorax. Due to the nature of the cosine calculation and the usage of the square root to determine the elevation angle, sign identification is lost. Thus the elevation angle will always be positive and will only range between 0° and 180°; if the angle exceeds this range, the larger, or smaller value will not be displayed. Since we are looking at a globographic representation, this calculation is acceptable (Figure 21). The latitude lines on one side of the globe should be equal to those on the other side.

Rotation in the elevated plane:

The plane of rotation was calculated by either:

$$\text{rotplane} = \arccos\ (\hat{e}_2 \bullet \hat{X}_t)$$

$$\text{rotplane} = \arcsin\ (\hat{e}_2 \bullet \hat{Y}_t)$$

This angle can be obtained by computing the angle between one of the segmental axes, X_t, of the thoracic coordinate system and the floating axis. By definition, the result of a cross product between two vectors produces a third vector perpendicular to the other two. Since the floating

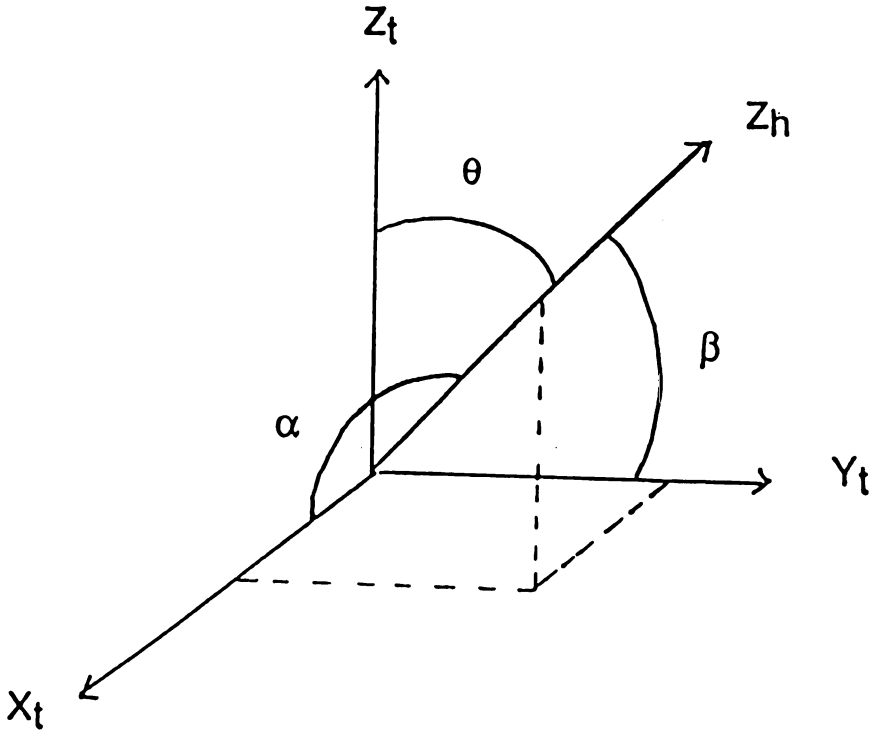

Figure 20: Spherical Angles

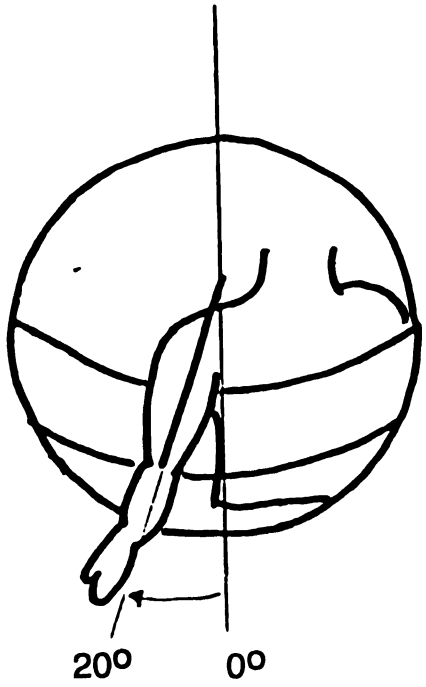

Elevation is measured by latitude lines

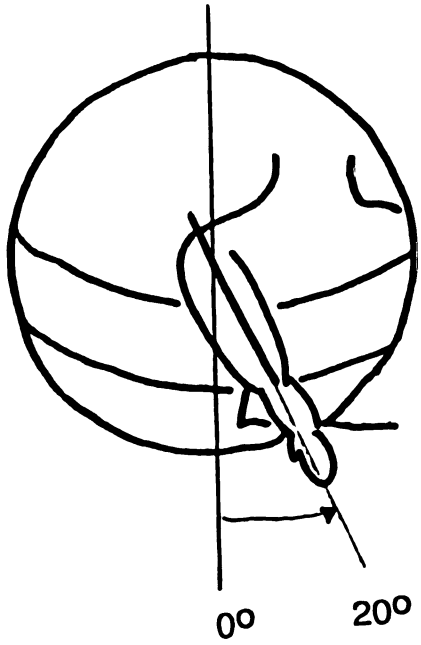

Figure 21: Elevation Angles

axis (e_2) is a cross product between Z_t and Z_h, e_2 is always perpendicular to both Z_t and Z_h and is in the thoracic XY plane. As described in the previous section, the rotation plane is the position of the arm as defined by the longitudinal lines on a globe centered around the glenohumeral joint.

When the floating axis is computed, it is in laboratory coordinates. The rotation angle in the elevated plane can be calculated from laboratory coordinates, but for ease of writing the computer algorithm the floating axis was transformed into the thoracic coordinate system.

$$\left[\vec{C}_{thor}\right]=[D]\left[\vec{C}_{lab}\right]$$

$$[D]=\begin{bmatrix} i_{xx}, i_{xy}, i_{xz} \\ i_{yx}, i_{yy}, i_{yz} \\ i_{zx}, i_{zy}, i_{zz} \end{bmatrix}$$

where $[D]$ is comprised of the axes of the thoracic coordinate system in the form of unit vectors:

$$\hat{X}_t = i_{xx}, i_{xy}, i_{xz}$$

$$\hat{Y}_t = i_{yx}, i_{yy}, i_{yz}$$

$$\hat{Z}_t = i_{zx}, i_{zy}, i_{zz}$$

After the transformation, the X,Y and Z axes of the thoracic coordinate system are used as references to identify the position of the floating axis. This position is then tracked from one frame to the next. When the floating axis is within 30 degrees of the zero degree angle, the arcsin calculation is

used to achieve a smooth curve through zero and to define the sign change of the angle.

Internal/External Rotation of the Humerus:

The internal/external rotation of the humerus was calculated in the following manner:

$$\text{inte} = \text{acos}(\hat{e}_2 \bullet \hat{X}_h)$$

$$\text{inte} = \text{asin}(\hat{e}_2 \bullet \hat{Y}_h)$$

As stated before, by the nature of the cross product, the floating axis is perpendicular to Z_h and Z_t and is therefore in the XY plane of the humeral coordinate system and in the XY plane of the thoracic coordinate system. This calculation was done in the same fashion as the rotation in the elevated plane except, the floating axis was left in the laboratory coordinate system.

The arcsin calculation was used to monitor a sign change and to produce a smooth curve through the zero angle.

Complications:

In both the rotation in the elevated plane and the internal/external rotation of the humerus, the direction of the floating axis was identified. Since the shoulder has a high range of motion, tracking of the floating axis was necessary. By slight movements in the neutral position, the floating axis can jump from quadrant to quadrant (Figure 22) which produces discontinuities. The problem occurs when the arm is at the side and forms a conical region where a slight adjustment of position causes the

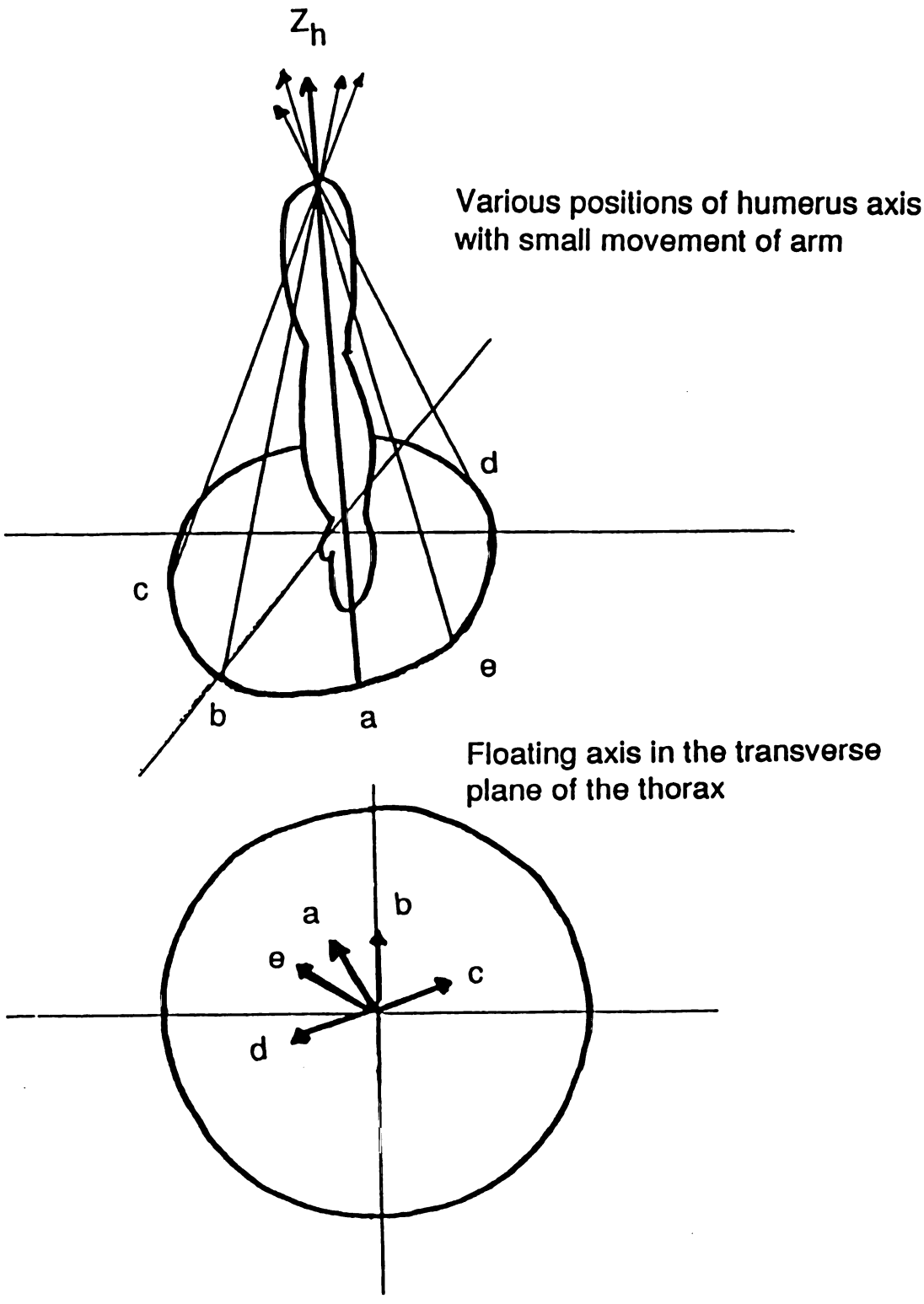

Figure 22: Conical Singularity Region

Z axis of the humerus and the Z axis of the thorax to cross. Since the floating axis is the cross product between these two axes, this causes a switch of axis direction, and maintaining the same cross product order causes the floating axis to jump to a different quadrant.

An index system was developed to identify the quadrant in which the floating axis was pointing and thus if any "jumping" of the floating axis occured, it was immediately identified. Then from this planar analysis, an index was assigned to the position of the floating axis, it's previous position is compared to its present position and then, the desired computation is performed.

It also should be noted that at the point where the Z axis of the humerus and the Z axis of the thoracic cage become parallel, the floating axis can no longer be defined. As these two axes approach this position, the accuracy of the cross product decreases. The data showed small gaps when this occurred, and points around the gap were scattered. The points around the gap were eliminated in a subjective fashion and thus created a larger gap, but cleaner data. Typically this happened at the initial starting position and in the externally rotated condition.

RESULTS

A collection of data obtained from the left arm of six different subjects is presented in this section. Data were processed for each trial and individual angles were plotted for each motion: elevation, the rotation in the elevated plane (rotation plane) and the internal/external rotation of the humerus. Representitive plots for the average subject and for a stocky subject are presented. The five thinner built subjects all had similar trends and ranges of motion, while the heavier, stocky subject had similar trends in the data but the ranges of motion were less. Because of this, the two sets of data are presented throughout this section. Data in the form of the individual angles, for the relaxed condition are presented in Figures 23 and 24. Data for the internally rotated humerus are presented in Figures 25 and 26. Data for the externally rotated condition are presented in Figures 27 and 28.

The overall ranges of motion for the three conditions based on different humeral rotations are comparable. None of the three different rotations showed a large change in motion when compared with the other two. A summary of the maximum ranges of motion for each humeral rotation condition are presented as follows in Table 2.

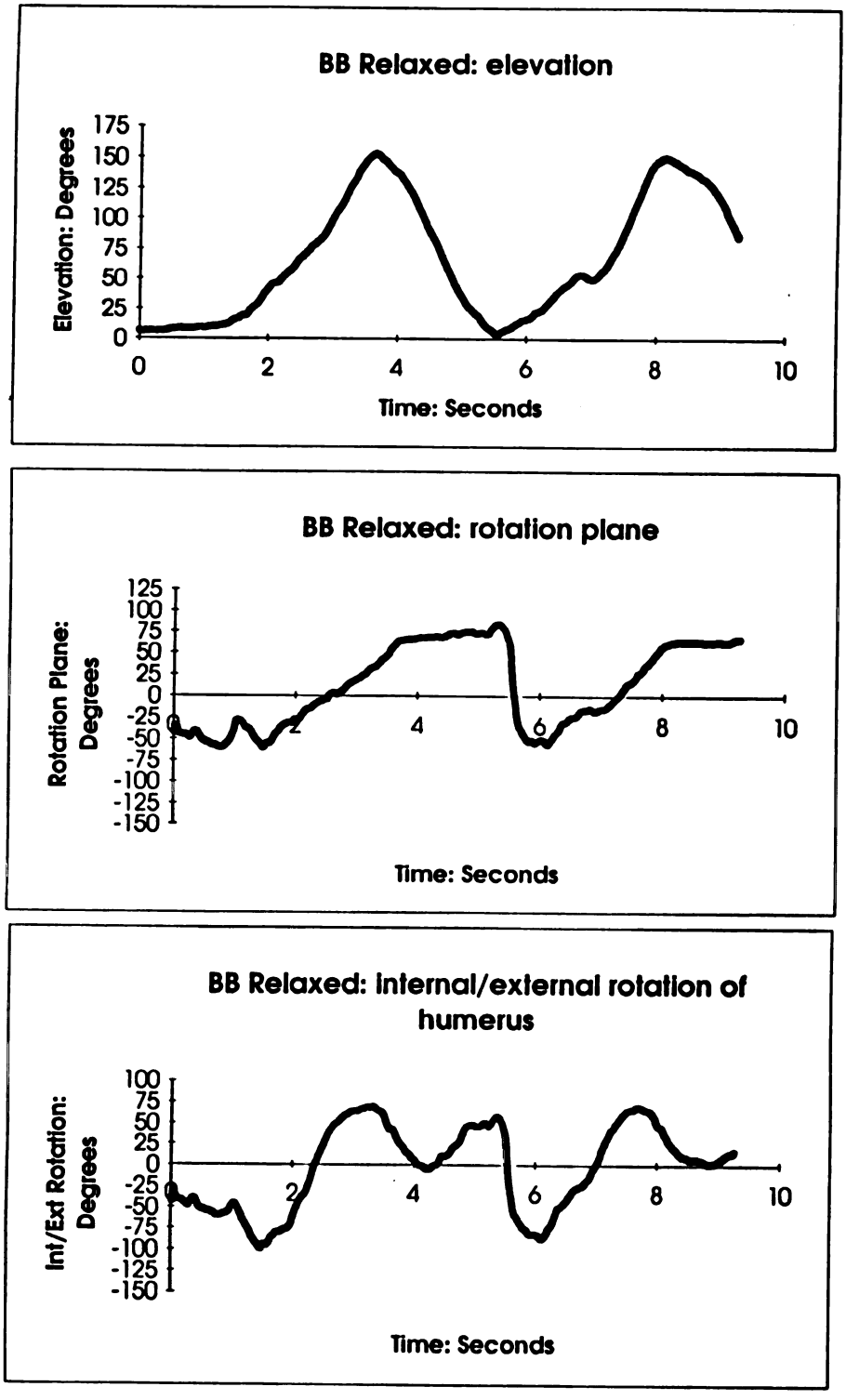

Figure 23: Range of Motion for Average Subject: Relaxed Condition

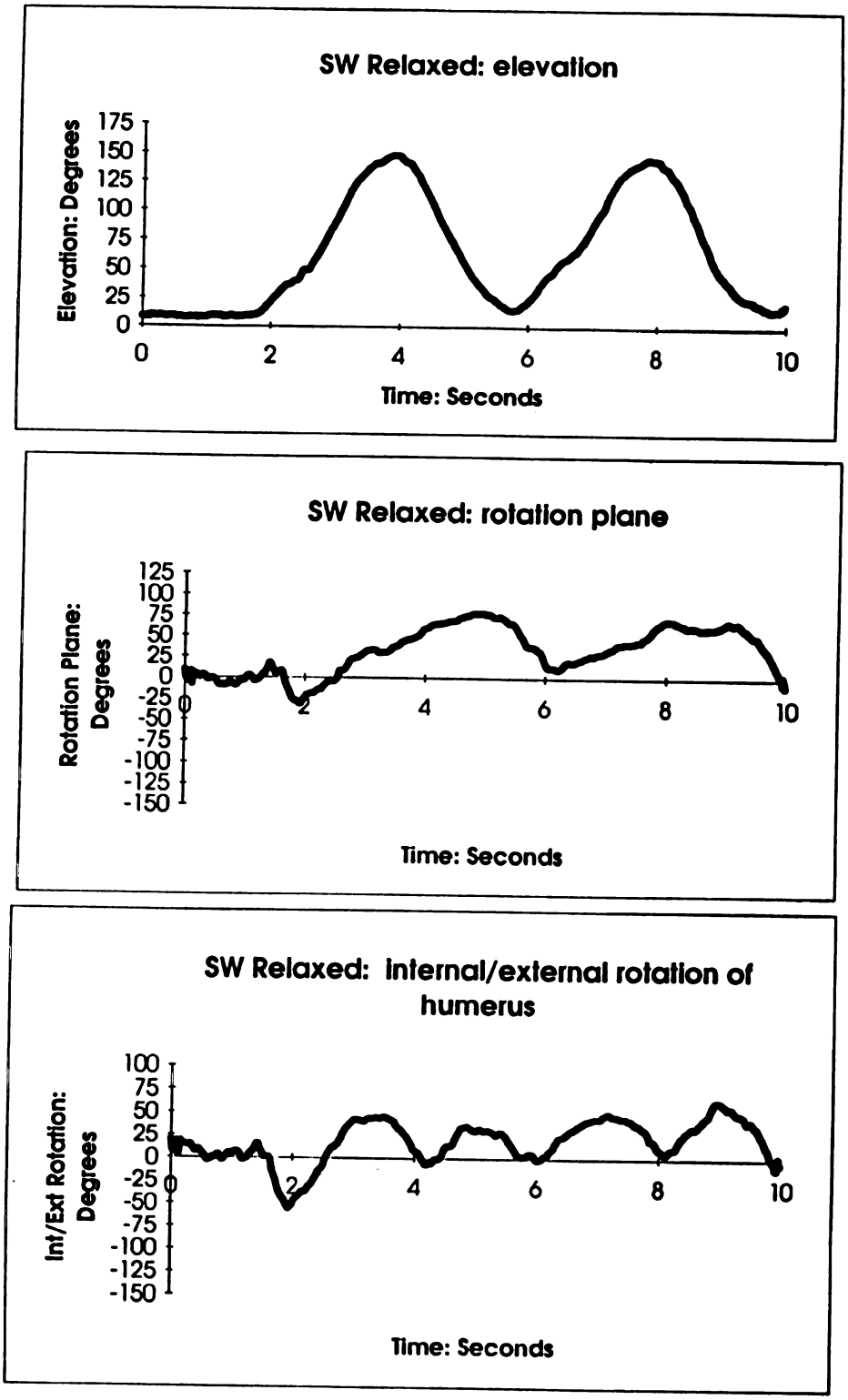

Figure 24: Range of Motion for Stocky Subject: Relaxed Condition

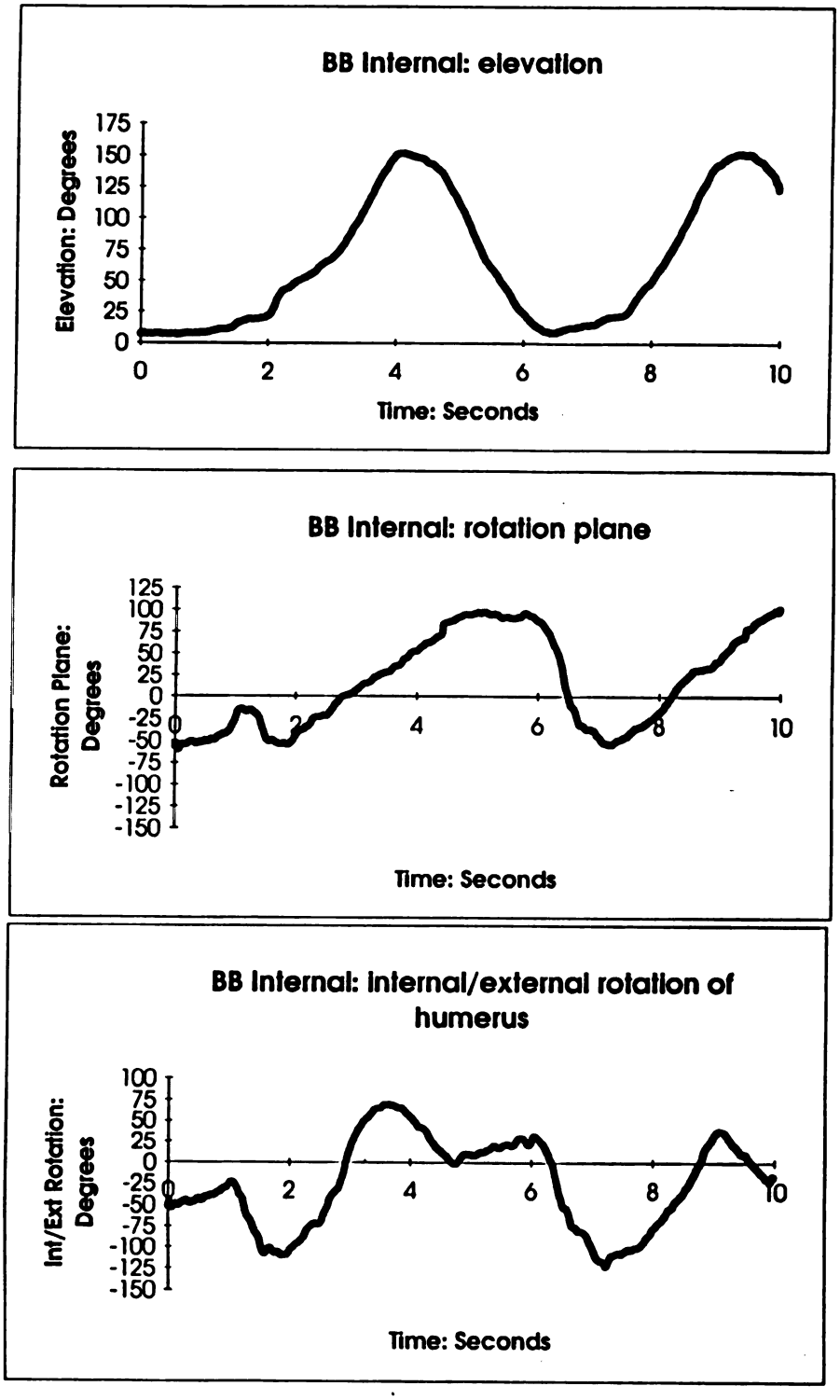

Figure 25: Range of Motion for Average Subject: Internal Condition

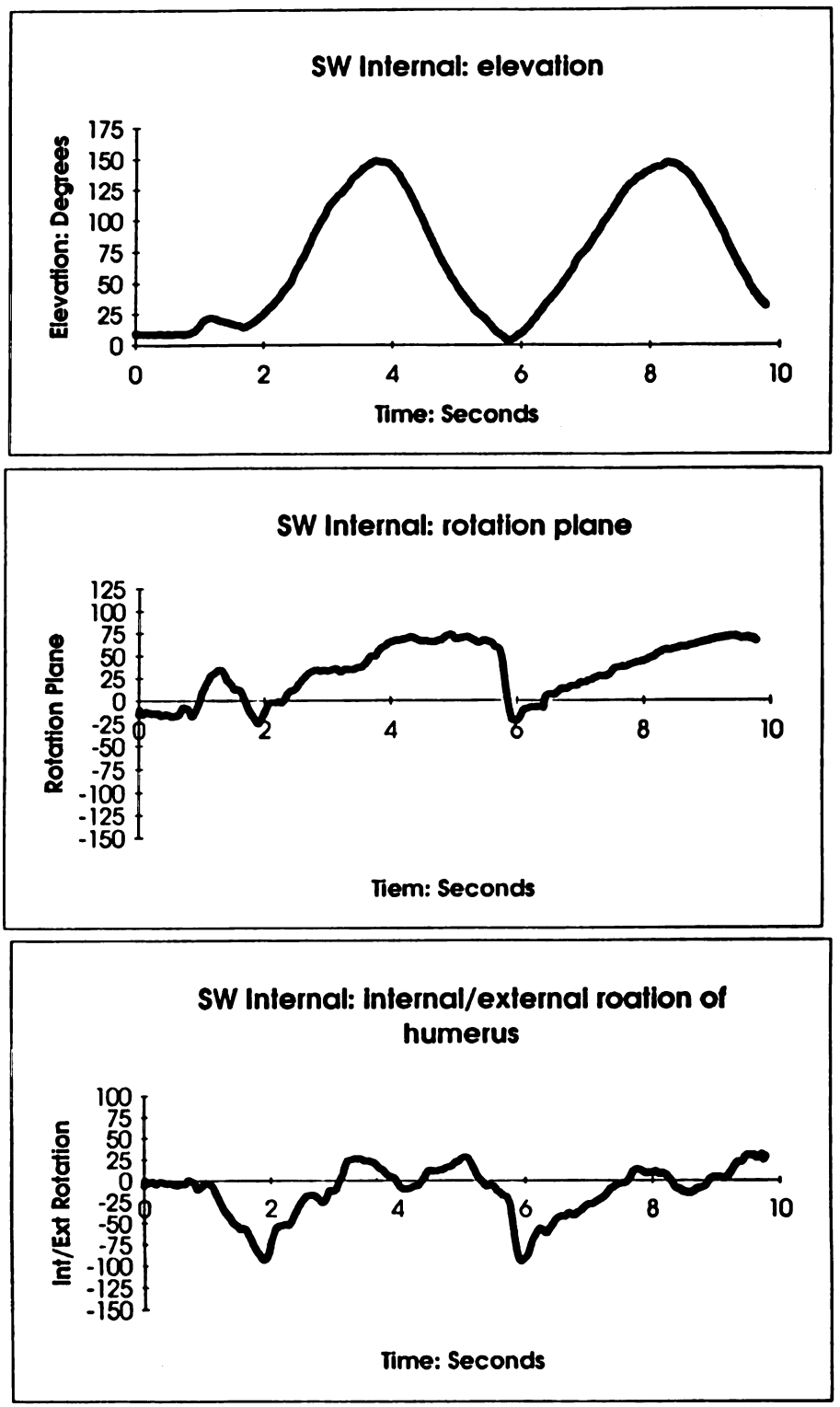

Figure 26: Range of Motion for Stocky Subject: Internal Condition

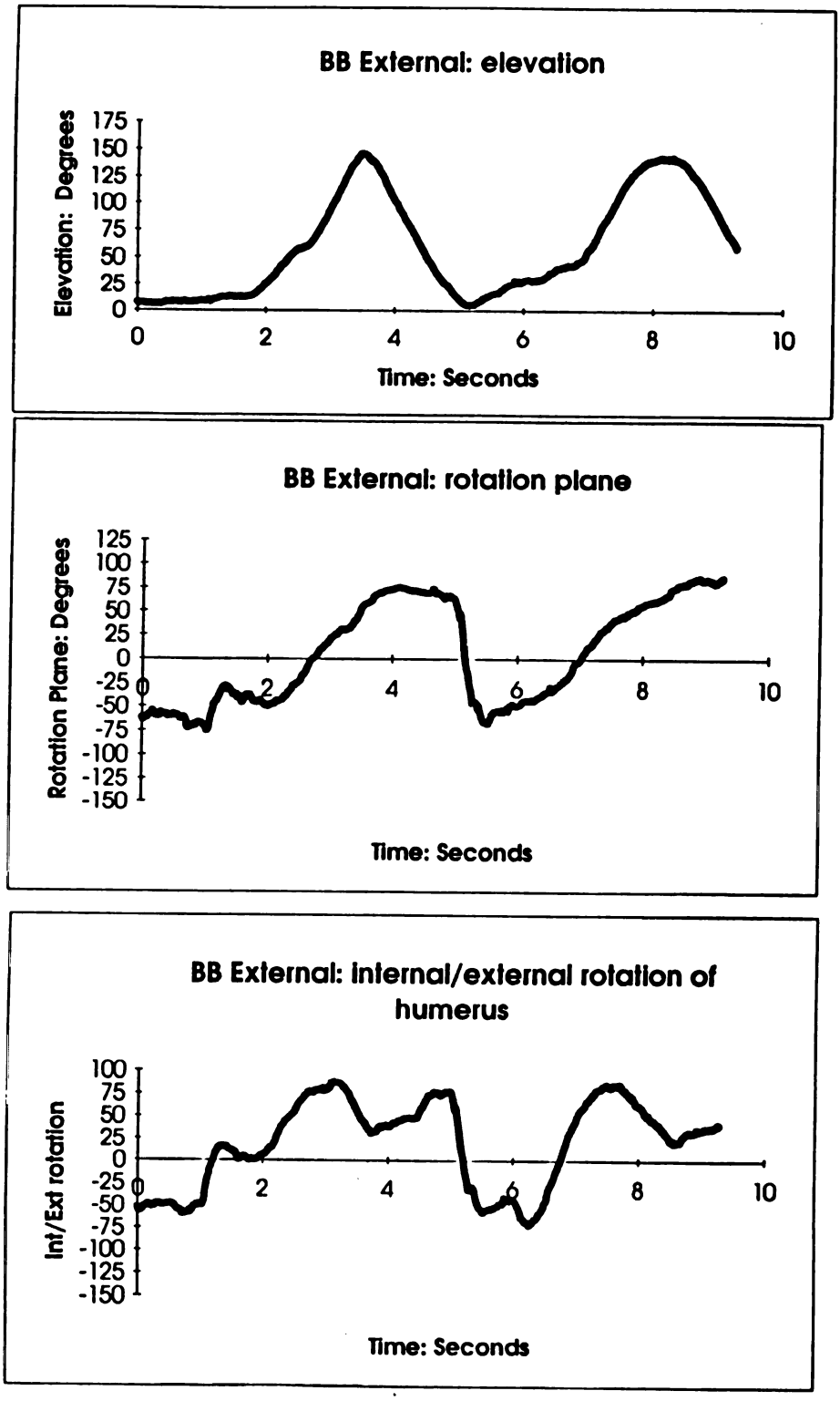

Figure 27: Range of Motion for Average Subject: External Condition

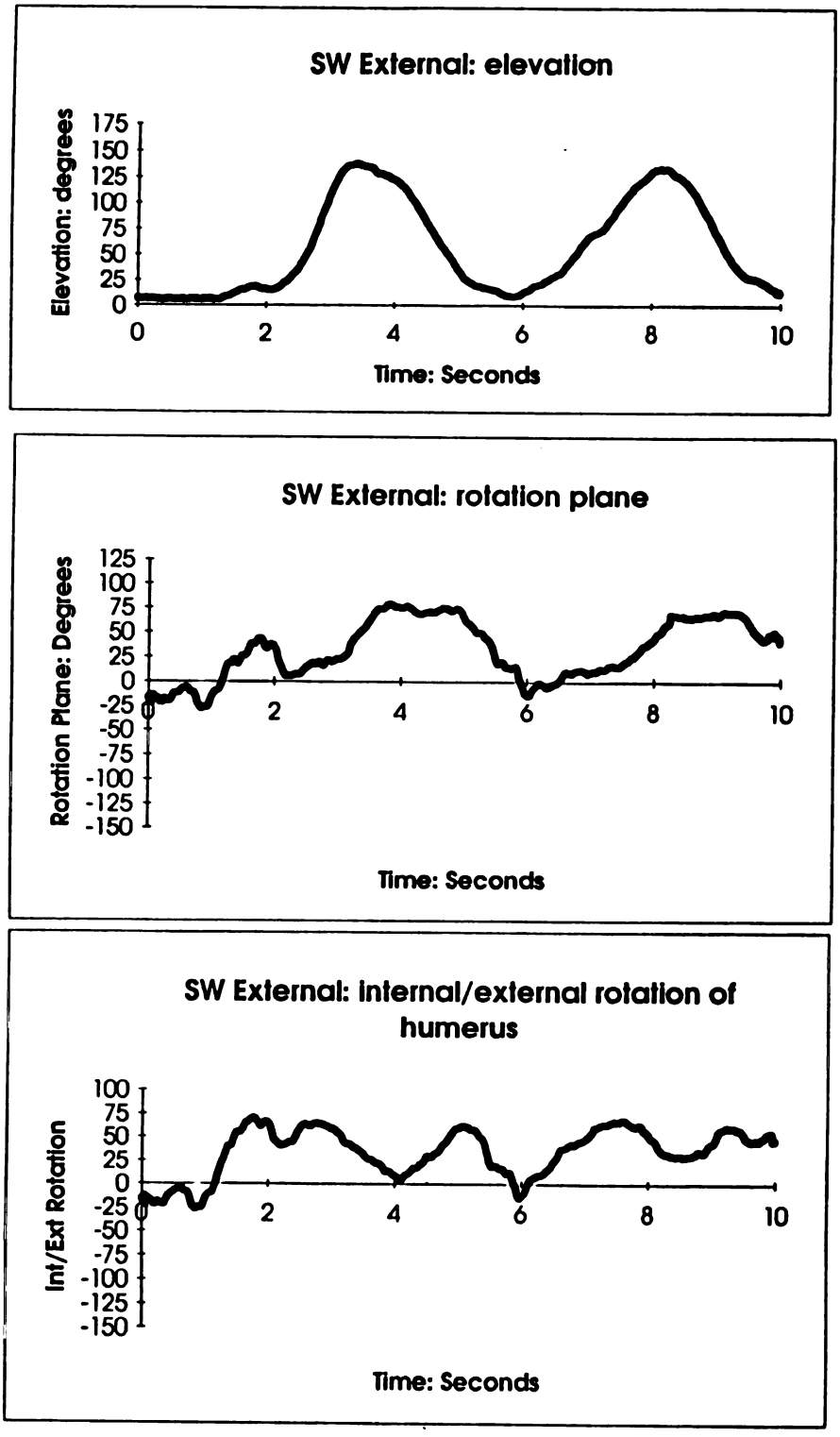

Figure 28: Range of Motion for Stocky Subject: External Condition

Table 2
Maximum Ranges of Motion

	Degrees Elevation	Degrees Rotation Plane	Degrees Int/Ext Rotation
Relaxed	131-153	108-207	97-186
Internal	121-151	98-193	133-201
External *	125-145	105-150	95-150

* Based on three subjects

For the relaxed condition, the subject with the lowest amount of elevation achieved the largest range of motion in the rotation plane and in the internal/external rotation of the humerus and the subject achieving the largest amount of elevation had the lowest range of motion in the two remaining angles.

Along with the individual angles, three sets of cross plots for each trial were then graphed:

1) rotation plane vs. elevation

2) internal/external rotation of the humerus vs. elevation

3) rotation plane vs. internal/external rotation of the humerus.

Figures 29 through 34 are representative trials with the subject BB having the average trend and ranges of motion while SW showed consistently the smallest overall ranges of motion. The data in Table 3 identifies the ranges of rotation in the elevated plane in which maximum elevation occurred. An average position in the rotation plane for all subjects was computed and is included in Table 3.

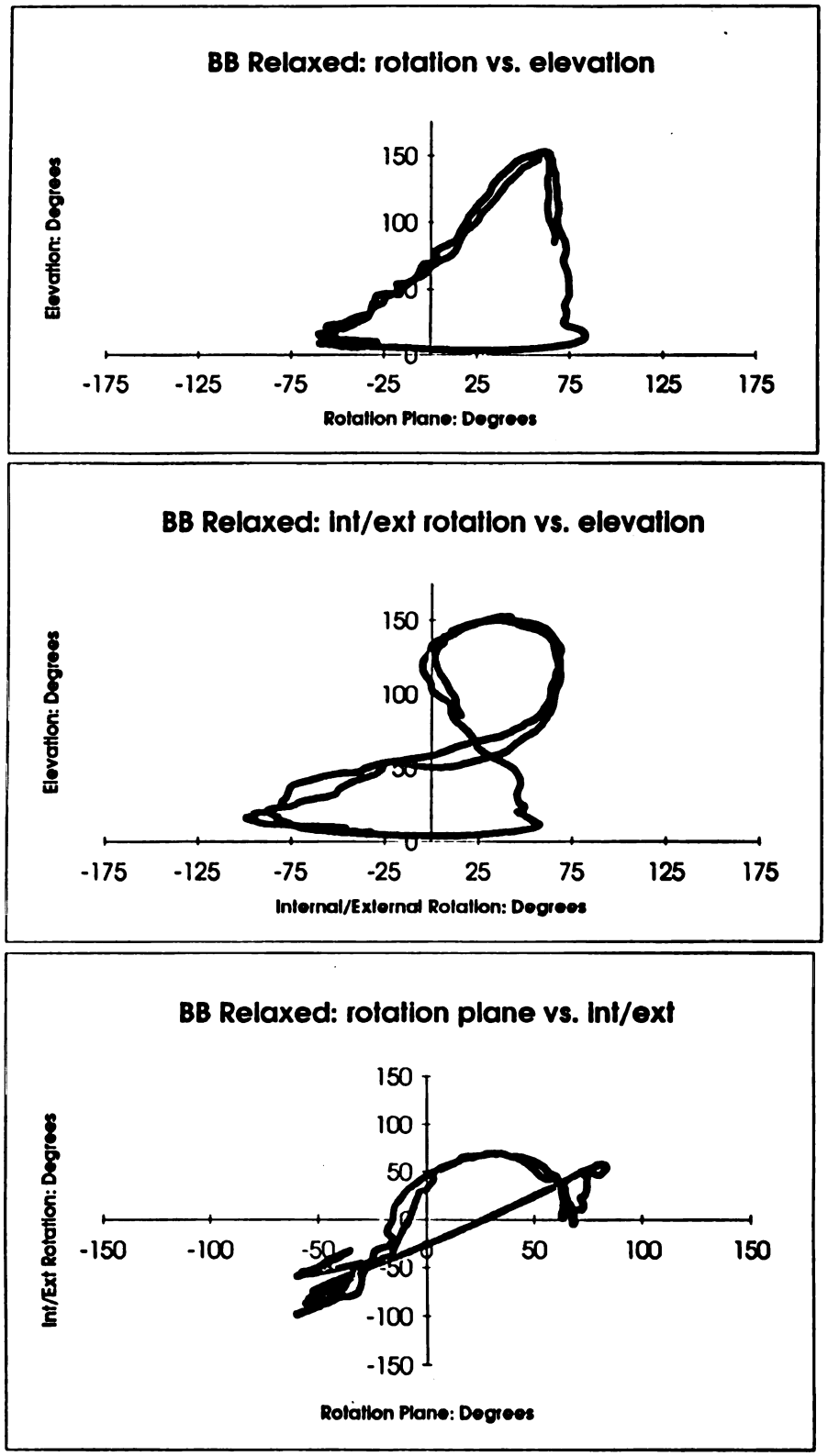

Figure 29: Cross Plots for Average Subject: Relaxed Condition

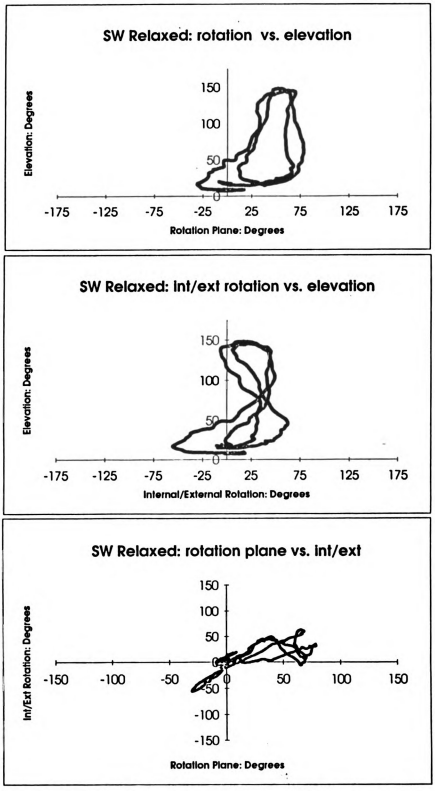

Figure 30: Cross Plots for Stocky Subject: Relaxed Condition

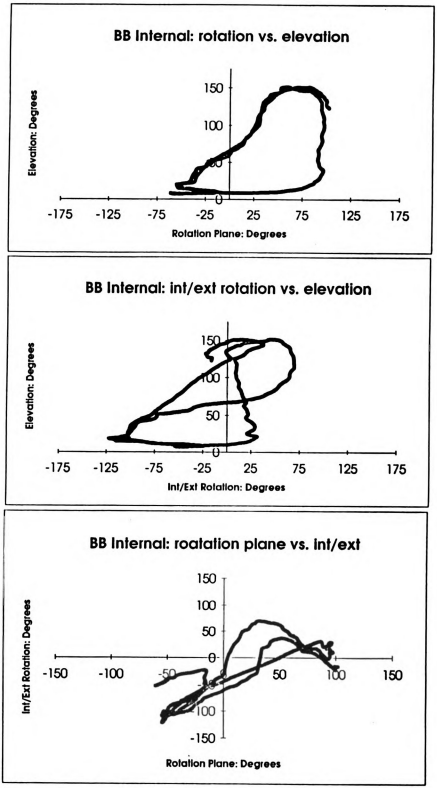

Figure 31: Cross Plots for Average Subject: Internal Condition

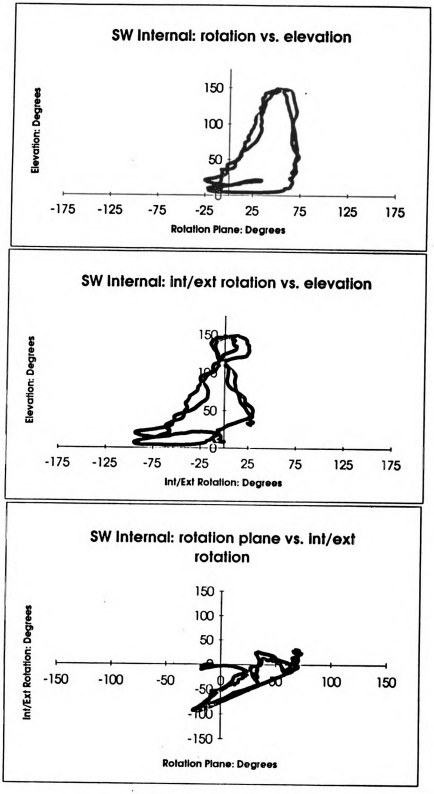

Figure 32: Cross Plots for Stocky Subject: Internal Condition

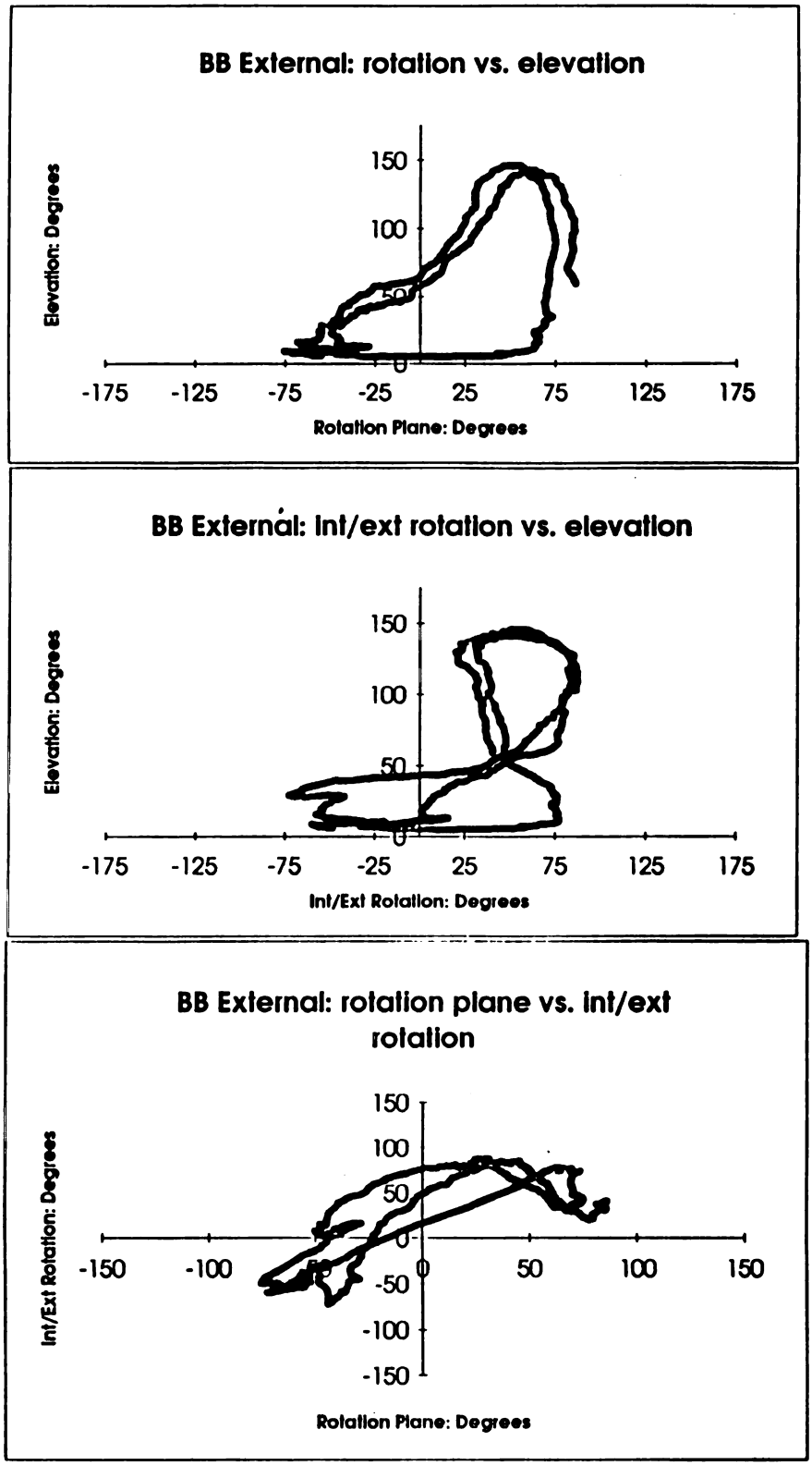

Figure 33: Cross Plots for Average Subject: External Condition

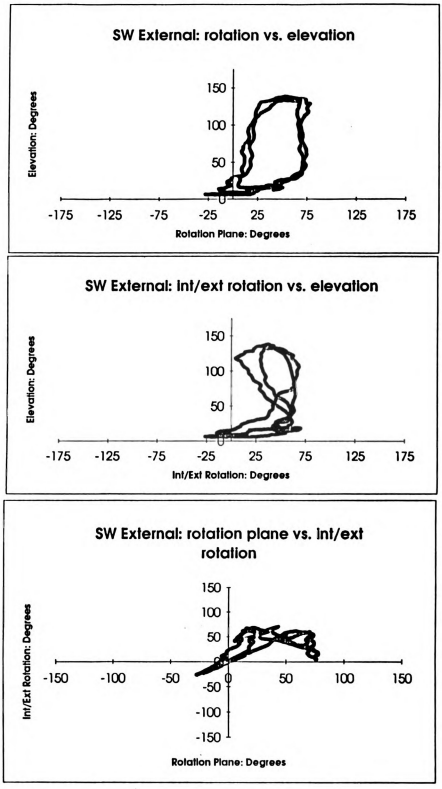

Figure 34: Cross Plots for Stocky Subject: External Condition

Table 3
Maximum Elevation vs. Plane of Rotation

	Degrees Elevation		Degrees Rotation Plane	
	Maximum	Average	Range	Average
Relaxed	153	142	38-75	57
Internal	151	140	40-80	66
External*	145	135	33-53	46

* Based on three subjects

The average elevation between conditons varied by 7 degrees and the maximum elevation angle occurred in the relaxed humeral roatation. The range of rotation was 11-20 degrees higher in the relaxed and internal humeral positions than in the external.

Summarized data from the second cross plot, the elevation vs. internal/external rotation of the humerus is presented in Table 4. The average amount of humeral rotation varied 31 degrees between the three different conditions. These graphs have some unique characteristics. One of the characteristics is that, during posterior elevation for the first half of the great circle completed by the prescribed motion and then during the lowering of the arm in the front of the body during the second half of the circle, there is a crossover point where the amount of humeral rotation is the same. This intersection is present in all plots and the ranges of this point are summarized in Table 5.

Table 4
Maximum Elevation vs. Internal/External Rotation

	Degrees Elevation		Degrees Int/Ext Rotation	
	Maximum	Average	Range	Average
Relaxed	153	142	20-72	41
Internal	151	140	10-50	35
External*	145	135	36-106	66

* Based on three subjects

Table 5
Intersection Point between Elevation and Humeral Rotation

	Degrees Elevation (Average)	Degrees Int/Ext Rotation (Average)
Relaxed	55	25
Internal	79	8
External*	46	56

* Based on three subjects

Notice the shift to the right of the intersection point, from the humeral rotation in the internal condition at 8°, to the humeral rotation in the external condition at 56°.

DISCUSSION

Little difference was observed in the ranges of the angles between the different humeral rotations. In the relaxed condition and the internal condition, an initial internal rotation can be observed, but then as the arm begins to move, it is forced to externally rotate (Figure 35 & 36). This is a natural motion, as one elevates the arm posteriorly and achieves a maximum rotation plane, the humerus is forced to externally rotated in order to continue the circular motion.

When comparing the cross plots obtained from these *in vivo* tests, to the cadaver tests obtained by An et al. (1), it was found that the maximum elevation range when the humerus was rotated in the external condition occurred between 33 and 53 degrees in the rotation plane which is anterior to zero degrees. The zero degree position occurs when the humeral Z axis is in the YZ plane or the frontal plane of the thoracic cage. When the humerus axis is in this position, the cross product between the Z axis of the thorax and the Z axis of the humerus creates a floating axis which is perpindicular to the frontal plane of the body. This is the 0° position as defined for this study. Each subject did not begin at 0°, but rather in the anatomically neutral position where the arm was for most subjects, slightly

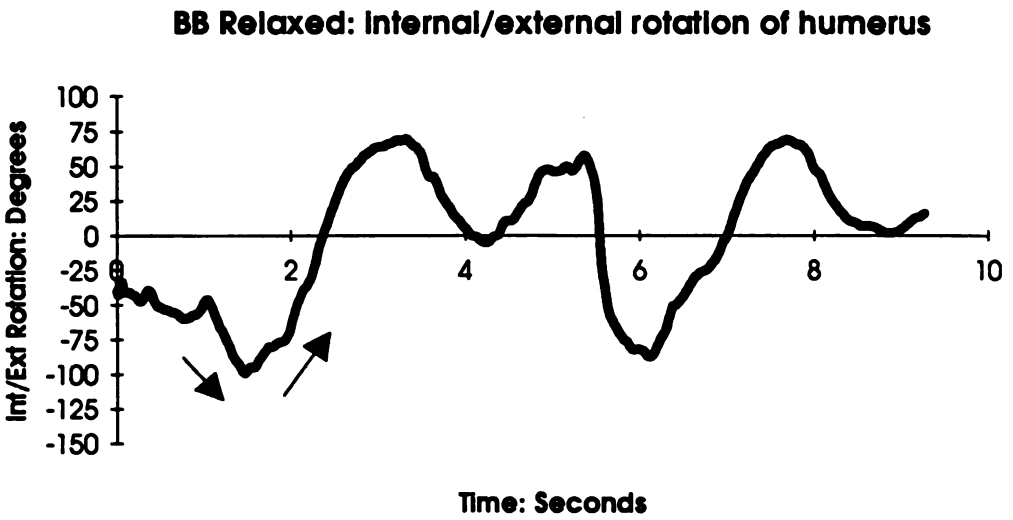

Figure 35: Humeral Rotation

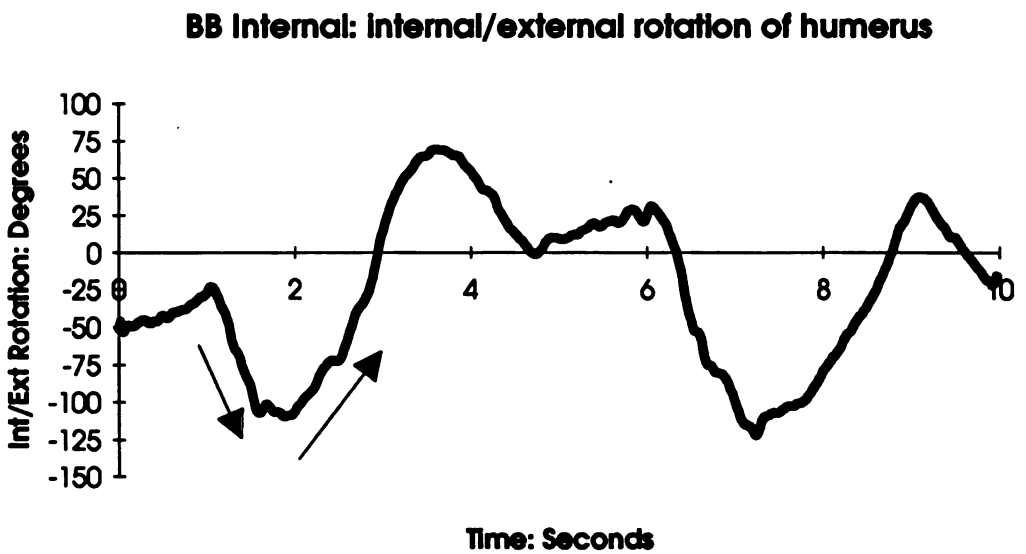

Figure 36: Humeral Rotation

posterior to the zero position. An et al. (1) found that the maximum elevation occurred at 25° anterior to the plane of the scapula when the humerus was rotated in the external position. The zero position in this study and the plane of the scapula are comparable, but are not necessarily equal. No physical measurements were taken to identify the plane of the scapula relative to the humerus and therefore, a physical verification cannot be made. The trends of the data are similar, with the amount of elevation being 20° higher and the rotation plane being 8°-28° larger in this *in vivo* experiment.

The maximum elevation relative to 0° for the internally rotated condition, occurred between 40° and 80° of rotation in the elevated plane and in the relaxed condition, the maximum elevation occurred between 38° and 75° of rotation in the elevated plane. As can be seen, the maximum elevation was produced within the same ranges of rotation in the elevated plane for all three positions of humeral rotation.

A second conclusion made by An et al. found that the maximum elevation posterior to the plane of the scapula occurred when the humerus was internally rotated. The data obtained in this research did not address this issue in the testing protocol and therefore could not be compared with the findings of An et al.. The primary objective was to obtain the largest range of motion at the glenohumeral joint in the global measurement system.

There are two major differences between the work done by An et al. and the research performed for this thesis. One was that this study was done *in vivo* while An et al. used cadaveric specimens and they could control the movements of the humerus. They were able to ensure that the humerus maintained the desired rotation either internally or externally by

fixing the position of the humeral bone. During this study, the subjects were not asked to wear any type of "locking brace" to maintain an external or internal rotation of the humerus, but were asked to maintain the desired position as best able throughout the test. As can be seen from the graphs, internal and external rotation of the humerus did occur.

A second difference was in the type of motions performed or induced on the subjects. An et al. selected planes of rotation and then elevated the humerus until it was restricted in the prescribed plane. They repeated this motion for several different planes of rotation and for conditions with the humerus internally rotated and externally rotated. For this research, an emphasis was not placed on the subject achieving the maximum amount of elevation in specific planes, but rather obtaining an overall maximum range of motion in the globographic sense. Because of these differences both in subjects and in motion formats some variation in the data are expected.

It was also felt that the relaxed condition would promote the largest overall range of motion. When analyzing the data, it was found that the relaxed condition did not consistently provide the maximum range of motion for all three angles. The maximum ranges of motions were mixed between all three conditions and all angles. No correlation could be established that one type of humeral rotation continually provided the maximum range of motion. It is felt that if the humerus was prevented from rotating in the internal and external conditions, then the relaxed condition would allow for the largest ranges of motion.

It should also be noted that the amount of fat, muscle or type of clothing worn during the testing procedure will affect the outcome of the data. Individuals wearing restrictive clothing, or who have large deltiod and trapezius muscle mass or are overweight may show a decrease in the

range of motion. Individuals which have muscles which are in pain may also show a decrease in their range of motion. None of the subjects used for this experiment were wearing any clothing on the thorax and none of the subjects exhibited any problem or pain in the shoulder region.

Five of the six subjects tested in this research were of thin build ranging in weight from 150 pounds at 5' 11" to 187 pounds at 6' 2" . The sixth subject was of a stocky build and had a height of 5' 11" and a weight of 199 pounds. This subject for all conditions showed the lowest range of motion in the plane of rotation and the internal/external rotation of the humerus, but not necessarily in elevation.

The second cross plot of elevation vs. internal/external rotation of the humerus has two unique characteristics. This plot has an overall shape similar to that of a figure eight with the lower half of the eight varying in size, followed by an intersection point (Figures 37& 38)

This intersection point may suggest that for this humeral rotation, there is an anatomical restriction on the amount of elevation which can be obtained both anterior and posterior to the body. Also note, that, between subjects and conditions, the lower half of the figure eight varies more in size and shape than does the upper half.

For the last cross plot of the rotation plane vs. internal/external rotation of the humerus, a rough linear relationship seems to exist between these two movements. This would also identify a coupling between these two motions.

These three cross plots have characteristics which, along with the evaluation of the range of motion might be a useful paramater in identifying

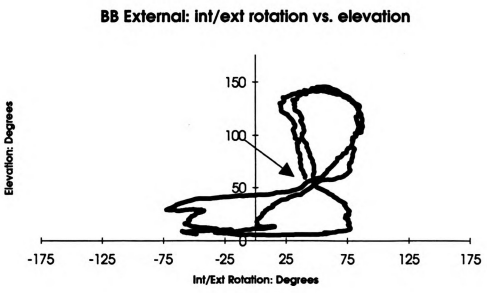

Figure37: Intersection Point

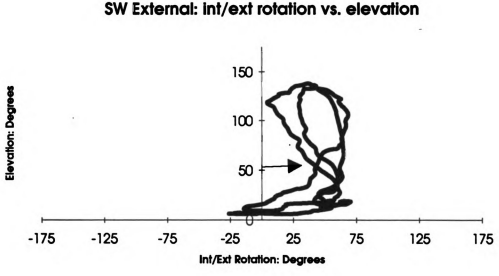

Figure 38: Intersection Point

the function or dysfunction of the shoulder joint. For example, the area under the curve along with the shape of the plot could be examined in the may be able to indicate a problem.

As discussed in the results section, the point of intersection gradually moves to the left as the condition changes from external to relaxed to internal while the amount of elevation at which this point occurs increases. This might also prove to be useful information in identifying shoulder dysfunciton.

BIBLIOGRAPHY

BIBLIOGRAPHY

1. An, K.N., Browne, A.O., Korinek, S., Tanaka,S., and Morrey, B.F. (1991) Three-Dimensional Kinematics of Glenohumeral Elevation. *Journal of Orthopaedic Research* 9:143-149.

2. Bechtol, C. O. (1980) Biomechanics of the Shoulder. *Clinical Orthopaedics and Related Research* 146:37-41.

3. Braune, W., Fischer, O., Amar,J., Dempster, W.T.(1963) Human Mechanics: Four Monographs Abridged. WADC Tech Report 63-123, Wright-Patterson Airforce Base, Ohio, Wright Air Development Center.

4. Cole G.K., Nigg, B.M., Ronsky, J.L. and Yeadon, M.R.(1993) Application of the Joint Coordinate System to Three- Dimensional Joint Attitude and Movement Representation: A Standardization Proposal. *Transactions of ASME* 115: 344-349

5. Dempster, W.T. (1965) Mechanisms of Shoulder Movement. *Archives of Physical Medicine and Rehabilitation* 46:49-70.

6. Dvir, Z. and Berme N. (1978) The Shoulder Complex in Elevation of the Arm: a Mechanism Approach. *Journal of Biomechanics* 11:219-225.

7. Engin, A. E. (1980) On the Biomechanics of the Shoulder Complex. *Journal of Biomechanics*13:575-590.

8. Engin, A.E. and Chen, S.M. (1986) Statistical Data Base for the Biomechanical Properties of the Human Shoulder Complex-: I: Kinematics of the Shoulder Complex. *Journal of Biomechanical Engineering.*108:215-221

9. Engin A.E. (1990omechanics of Diarthrodial Joints. Mow,Ratcliffe and Woo, Springer-Verlag. 405-439.

10. Engen, T.J. and Spencer, W.A. (1968) Method of Kinematic Study of Normal Extremity Movements. *Archives of Physical Medicine and Rehabilitation* 49:9-12.

11. Feltner, M. Dapena J. (1989) Three-Dimensional Interactions in a Two-Segment Kinetic Chain. Part I: General Model. *International Journal of Sport Biomechanics* 5:403-419

12. Grood, E.S. and Suntay,W.J. (1983) A Joint Coordinate System for the Clinical Description of Three-Dimensional Motions: Application to the Knee. *Transactions of the ASME* 105:136-144.

13. Hogfors, C., Peterson, B., Sigholm G. and Herberst, P. (1991) Biomechanical Model of the Human Shoulder Joint- II. The Shoulder Rythm. *Journal of Biomechanics* 24:699-709

14. Inman, V.T., Saunders, J.B., and Abott, L.C.(1944) Observations on the Function of the Shoulder Joint. *Journal of Bone Joint and Surgery* 26A:1-30.

15. Joint Motion Method of Measuring and Recording. (1965) American Acadamy of Orthopaedic Surgeons

16. Moore,Keith L. (1992) Clinically Oriented Anatomy . Williams and Wilkins, Baltimore, MD.

17. Miyazaki S. and Ishida A. (1991) New Mathematical Definition and Calculation of Axial Rotation of Anatomical Joints. *Transactions of the ASME* 113:270-275

18. Product Bulletin for 3M High Gain 7610 and High Contrast 7615. (1993) Industral Optics/3M, St. Paul, Minnisota.

19. Sakurai, S., Ikegami, Y., Okamoto, A., Yabe, K. and Toyoshima, S. (1993) A Three-Dimensional Cinematographic Analysis of Upper Limb Movement During Fastball and Curveball Baseball Pitches. *Journal of Applied Biomechanics* 9:47-65.